NASA TN D-900

TECHNICAL NOTE

D-900

AERODYNAMIC LOAD MEASUREMENTS AND OPENING CHARACTERISTICS OF AUTOMATIC LEADING-EDGE SLATS ON A 45° SWEPTBACK WING AT TRANSONIC SPEEDS

By Donald D. Arabian, Jack F. Runckel,
and Charles F. Reid, Jr.

Langley Research Center
Langley Field, Va.

NATIONAL AERONAUTICS AND SPACE ADMINISTRATION

WASHINGTON

September 1961

1Z

NATIONAL AERONAUTICS AND SPACE ADMINISTRATION

TECHNICAL NOTE D-900

AERODYNAMIC LOAD MEASUREMENTS AND OPENING CHARACTERISTICS OF AUTOMATIC LEADING-EDGE SLATS ON A 45° SWEPTBACK WING AT TRANSONIC SPEEDS[1]

By Donald D. Arabian, Jack F. Runckel,
and Charles F. Reid, Jr.

L
1
6
0
9

SUMMARY

Measurements of the normal force and chord force were made on the slats of a sting-mounted wing-fuselage model through a Mach number range of 0.60 to 1.03 and at angles of attack from 0° to 20° at subsonic speeds and from 0° to 8° at Mach number 1.03. The 20-percent-chord tapered leading-edge slats extended from 25 to 95 percent of the semispan and consisted of five segments. The model wing had 45° sweep, an aspect ratio of 3.56, a taper ratio of 0.3, and NACA $64_{(06)}$A007 airfoil sections. Slat forces and moments were determined for the slats in the almost-closed and open positions for spanwise extents of 35 to 95 percent and 46 to 95 percent of the semispan.

The results of the investigation showed little change in the slat maximum force and moment coefficients with Mach number. The coefficients for the open and almost-closed slat positions had similar variations with angle of attack. The loads on the individual slat segments were found to increase toward the tip for moderate angles of attack and decrease toward the tip for high angles of attack. An analysis of the opening and closing characteristics of aerodynamically operated slats opening on a circular-arc path is included.

INTRODUCTION

Thin swept wings have been used to advantage in delaying the effects of compressibility in the transonic speed range. The flow over these wings usually separates first in the tip region at relatively low values of lift coefficient, and the separation progresses inboard with increasing lift coefficient. The resultant effect is a decrease in the longitudinal

[1]Supersedes declassified NACA Research Memorandum L53I30 by Donald D. Arabian, Jack F. Runckel, and Charles F. Reid, Jr., 1954.

stability and an increase in drag. In an attempt to alleviate these undesirable characteristics, several types of auxiliary devices have been incorporated on the leading edges of sweptback wings. One of the most promising of these devices is the leading-edge slat. Leading-edge slats have been shown to increase the lift coefficient and lift-drag ratio and to decrease drag coefficient at moderate angles of attack and to extend the lift coefficient at which pitch-up occurs (refs. 1 and 2). Extension of the linearity of the longitudinal- and lateral-stability-derivative curves to higher angles of attack with slats open was shown in reference 3. These improvements can be attributed to the reduction of separation present at moderate angles of attack by the injection of flow into the boundary layer of the upper surface through the slat gap and to the interruption of the spanwise boundary-layer flow by the trailing vortex from the inboard edge of the slat. In general, these changes in the aerodynamic characteristics would improve maneuvering at both high and low speeds and at moderate and high angles of attack.

In addition to the effects of the slats on the airplane aerodynamics, a knowledge of the loads on the slats themselves is necessary in order to provide a structurally safe and, in the case of automatic slats, smoothly operating design. Available information on slat loads for swept wings at low subsonic speeds can be found in references 4 to 7. Either pressure or force measurements, or both, on various slat configurations at high-subsonic speeds are given in references 1 and 8 to 10. The present paper extends the scope of slat-loads information to the transonic speed range.

A wing-fuselage model, which had a 45° sweptback wing incorporating leading-edge slats, was tested in the Langley 16-foot transonic tunnel to determine the forces and moments on the slats in the open and almost-closed positions for slats of two spanwise extents. The loads on the individual slat segments, the total slat loads, and the opening and closing characteristics of the slats are presented for Mach numbers of 0.60 to 1.03 and angles of attack from 0° to 20° at subsonic speeds and from 0° to 8° at Mach number 1.03.

SYMBOLS

C_N slat normal-force coefficient, $\frac{\text{Slat normal force}}{qS}$, positive values up, perpendicular to wing chord line

C_C slat chord-force coefficient, $\frac{\text{Slat chord force}}{qS}$, positive values rearward, parallel to wing chord line

C_m slat moment coefficient about the slat rotation point, $\frac{\text{Slat moment}}{qS\bar{c}}$, positive values indicate tendency for slat leading edge to rotate up

C_R slat resultant-force coefficient, $\sqrt{C_N^2 + C_C^2}$

S slat area, projection on slat chord plane, sq ft

b/2 semispan, ft

c slat chord perpendicular to the wing 13-percent-chord line (coincident with wing chord line in the closed position), ft

$\bar{c}$ slat mean aerodynamic chord, ft

c' wing chord perpendicular to wing 13-percent-chord line (see fig. 2)

L/D lift-drag ratio

M free-stream Mach number

q incompressible dynamic pressure, lb/sq ft

P pressure coefficient, $\frac{p_l - p}{q}$

p_l local static pressure, lb/sq ft

p free-stream static pressure, lb/sq ft

$\frac{x_p}{c}$ position of intersection of resultant-force vector along slat chord line, fraction of slat chord

$\frac{X}{c}$ distance of slat rotation point behind wing leading edge, parallel to wing chord line (see fig. 14), fraction of slat chord

$\frac{Y}{c}$ distance of slat rotation point below wing chord line, perpendicular to wing chord line (see fig. 14), fraction of slat chord

r radial extension (fig. 14), ft

α model angle of attack, deg

θ direction angle of slat resultant-force vector from wing chord line, $\tan^{-1}\frac{C_N}{C_C}$

C_D model drag coefficient

C_L model lift coefficient

C_{m_A} model pitching-moment coefficient about 0.35 of wing mean aerodynamic chord

Subscript:

s slat segment

MODEL AND APPARATUS

Figure 1 is a photograph of the model mounted in the Langley 16-foot transonic tunnel. The model, which was tested without horizontal or vertical tail during this investigation, was attached to the sting-support system by a six-component internal strain-gage balance. A sketch of the model and slat arrangement is shown in figure 2. The wing had 45° sweep at the quarter-chord line, an aspect ratio of 3.56, a taper ratio of 0.3, and NACA $64_{(06)}$A007 airfoil sections streamwise. The aluminum-alloy tapered slats had a chord length of 20 percent of the local streamwise wing chord and were divided into five spanwise segments which extended from 25 to 95 percent of the wing semispan. In the closed position, the slats were sealed at the trailing edge, although a small gap existed on the undersurface between the slat and the wing proper (fig. 3). Each slat segment was extended forward perpendicular to the wing 13-percent-streamwise-chord line and was secured to the wing by two beams; various slat positions were obtained by changing these beams, as shown in figure 3. Each beam in the left wing was connected to a three-component strain-gage balance mounted internally in the wing. These balances measured one chordwise and two normal components of the slat-segment load with respect to the wing chord line.

The orientation of the slat in the almost-closed and open positions was determined by moving the slat along a circular-arc path, the center of which was located 262 percent of the local slat chord below the wing chord line and 63 percent of the local slat chord behind the leading edge of the slat in the closed or retracted position. The slat configurations and positions for which slat-load data were obtained are given in the following table:

Slat geometric characteristics					
Span extent, percent semispan	Segment numbers	Position	Deflection angle, deg	Gap, percent slat chord	Extension, percent slat chord
25 to 95	1, 2, 3, 4, 5	Almost closed	1.25	2.5	5.0
35 to 95	2, 3, 4, 5	Open	10.10	19.0	45.0
46 to 95	3, 4, 5	Open	10.10	19.0	45.0

Slat loads could not be measured in the closed position because some clearance was necessary between the wing and slat for free operation of the strain-gage balances. For this reason a small clearance was allowed for the tested position and this configuration is referred to as the "almost-closed" position. This almost-closed position with unsealed slots was representative of the slat leaving or returning to the closed position during automatic operation.

Pressure data were obtained from groups of three chordwise pressure orifices installed at five spanwise stations on the surface of the wing beneath the slats as shown in figure 2.

TESTS AND REDUCTION OF DATA

The tests were conducted in the Langley 16-foot transonic tunnel, a full description of which is given in reference 11. Slat loads were investigated through a range of Mach number from 0.60 to 1.03 for an average Reynolds number range from 5.5×10^6 to 6.7×10^6 based on the wing mean aerodynamic chord. The model angle of attack was varied from 0° to 20° for Mach numbers less than 1.00, whereas the maximum angles of attack for Mach numbers of 1.00 and 1.03 were 11° and 8°, respectively. Six-component model force and moment data and underslat pressures were obtained simultaneously with the slat-force data. A few of the slat-force-data points were repeated, all of which are presented in the slat-segment plots. The noticeable differences of some of the repeat points near the peak loads may be attributed to possible instability at the stall.

Corrections were applied to the slat-force data for balance interaction effects and temperature changes. No correction was made, however, for the weight shift of the slats due to angle-of-attack change, because this error

was found to be less than 1 percent at 20° angle of attack. The forces on the individual slat segments were computed by summing the respective components of the two balances supporting each segment; the moment on each segment was taken about the slat center of rotation. No correction was made to the data for tunnel-wall interference inasmuch as it was shown in reference 12 to be small. No evidence of boundary-reflected disturbances affecting the data was found.

Slat-Segment Characteristics

The leading-edge slat of the present investigation was divided into 5 spanwise segments (fig. 2) in order to determine the effect of slat spanwise extent on slat opening characteristics and on the model aerodynamic characteristics with the slats open. The almost-closed configuration, in which the slats were displaced outward slightly from the closed position, allowed some air to flow through the slot passage. Slat-segment force and moment coefficients C_{N_s}, C_{C_s}, and C_{m_s} for all five spanwise segments in the almost-closed position are presented in figure 4 as a function of angle of attack and Mach number. The effect of Mach number on all slat segment maximum force coefficients was usually small. For all Mach numbers the normal-force-coefficient curves indicate a general increase in slope with increase in segment distance from the fuselage center line at low angles of attack. However, the force break occurs first on the outermost segments at moderate angles of attack. With increasing angle of attack the maximum load progressed inboard, with the result that the peak load occurred at the inboard segment at the highest angles of attack. Similar change in the spanwise loads in the vicinity of the leading edge of plain swept wings was indicated from test data of references 8 and 13. Measurements of the underslat pressures of the 25- to 95-percent-semispan slats in the almost-closed position (fig. 5(a)) showed a greater pressure increase on the slat segments at the wing tip than on those inboard up to about $\alpha = 7°$. This pressure increase would thus contribute to the greater slope of the normal-force-coefficient curves at the tips. The underslat pressures of the open slat indicate no tendency to increase toward the tip (fig. 5(b)).

The opening and closing characteristics of the slats are determined from the moment-coefficient curves. A positive slat moment about the slat center of rotation tends to rotate the slat closed or to hold it in a closed position, whereas a negative moment tends to open the slat or to hold it in the open position. A zero moment coefficient indicates that the slat is on the verge of either opening or closing. The zero-moment angle of attack for the almost-closed position of the slat segments shows that the segments will open in succession with increasing angle of attack, beginning with the tip segment. The inboard segment lagged the adjacent segment by as much as 5°. The lag of the inboard segment can be explained by the plan-form shape. The streamwise position of the inner edge

distributes the area, and thus the load, further ahead of the moment axis causing a more positive moment which tends to delay opening. Since in an actual installation the slat would not be segmented, this tendency for the inboard portion to remain closed would be undesirable; for this reason this segment was not tested in the open position.

The force and moment coefficients for the opened slat segments are shown in figures 6 and 7 for the 35- to 95- and 46- to 95-percent-semispan slat extents, respectively. In general, the variation of the coefficients with angle of attack for the opened slat segments are similar to those discussed for the segments in the almost-closed position except for a displacement of the curves to about 3° or 4° higher angle of attack. This displacement may be explained by the fact that, in the extension process, the slats are deflected downward and translated forward which changes the angle-of-attack reference and the induced angle of attack of the slat such that the zero force coefficients should occur at higher angles of attack.

In the discussion of the almost-closed slats, it was pointed out that the inboard segment (segment number 1; fig. 2) lagged the adjacent segment excessively. The inboard segment in the extended position (segment number 2) also lagged the adjacent segment, but the lag was reduced. Apparently, the lag was affected by spanwise position of the segment and end effect as well as plan-form shape, but the contribution of each is not known. The results of the slat-segment-load investigation are in good agreement with unpublished data from another facility obtained at Mach numbers of 0.60, 0.85, and 0.90.

Total-Slat Characteristics

The force and moment coefficients of the individual slat segments were combined into total-slat coefficients to show the integrated effect of the segments. The total-slat coefficients are shown in figure 8 for the 35- to 95-percent-semispan slat and the 46- to 95-percent-semispan slat in the open and almost-closed positions. The almost-closed total-slat coefficients were obtained by combining only the segments necessary to make up these two spanwise extents from the almost-closed-slat data. No adjustment was made for the end effect of the innermost segment, which would tend to shift the curves of figure 8 to about 0.5° lower angle of attack. The characteristics of the slats in the open and closed positions are similar except for a shift of the zero force coefficient to about 4° higher angle of attack for the open slats.

Reducing the span of the open slats from 35- to 95-percent semispan to 46- to 95-percent semispan caused a slight shift in all the force-coefficient curves to lower angles of attack, but the magnitude of the peak values of force coefficients remained about the same. The zero

moment coefficients also were changed such that the angle of attack at which the slats started to close was about 1° lower for the 46- to 95-percent-semispan slats and the opening angle was about 0.5° lower.

The variation of the normal-force coefficient with the chord-force and the moment coefficients is shown in figure 9 for Mach numbers of 0.85 and 1.00. The variations of the coefficients are approximately linear from normal-force coefficients of about 0 up to normal-force coefficients where separation was expected to exist on the slat, or up to the test limit at Mach numbers of 1.00 and higher. This linearity prevailed for all Mach numbers tested. The chord force at moderate and high angles of attack acted in the thrust direction.

The changes of the total-slat coefficients with angle of attack were similar for all Mach numbers in both closed and open positions. Maximum force coefficients usually decreased slightly with increasing Mach number.

Effect of the Resultant-Force Vector on the Kinematics of the Slat

For simulated automatic operation, the kinematics of the slat is determined by the location of the resultant of the slat aerodynamic loads. Figure 10 shows the effect of slat position on the slat resultant-force coefficient and the angle θ, measured counterclockwise from the wing chord line to the resultant vector, for 35- to 95-percent-semispan slats. The location of the intersection of the resultant-force vector with the slat chord line for the same configuration is shown in figure 11. It should be noted that in previous figures, force coefficients were measured with respect to the wing chord line rather than the slat chord line for both open and closed slat positions. Because the differences in force characteristics for the 35- to 95- and the 46- to 95-percent-semispan slats are relatively small, the resultant characteristics for the 46- to 95-percent slats will be similar to the curves shown.

It may be seen from figures 10 and 11 that the greatest changes in the location and angle of the slat resultant force occur at angles of attack from 0° to about 8°, and therefore, from a mechanical viewpoint, the operation of aerodynamically operated slats should be confined to this region. Where no changes in the location and direction of the slat force vector occur with angle of attack, no simple mechanism will operate the slats satisfactorily even though the vector magnitude may be changing with angle of attack.

Some alteration of the slat resultant characteristics is possible by changing the underslat pressures. This change may be accomplished by sealing the trailing edge of the retracted slat to the wing, which would move the center of pressure rearward for the closed slats and cause them to open at a lower angle of attack. Diverging the walls of the slot

between wing and slat would tend to have a similar effect. Sealing the lower surface of the slat or converging the slot would result in an opposite tendency.

Relation of Slat Position to Model Aerodynamic Characteristics

Six-component model force and pitching-moment data (ref. 14) for the slats-open and slats-closed configurations were compared to show the effect of the open slats on the model aerodynamic characteristics. The difference between the model force data for the open and closed slats is shown in figure 12. Positive differences indicate an increase in C_L, L/D, and C_D. The difference of pitching-moment coefficients indicates the pitching increments caused by opening the slats; a positive difference is a greater nose-up moment for slats open. In general a more stable condition exists for the slats-open configuration up to an angle of attack of about 10°.

For the Mach number range tested, the C_L and L/D increments became positive at angles of attack from 6.5° to 8°, whereas the C_D increment became negative. The L/D increment becomes fairly constant at high angles of attack for all Mach numbers, but otherwise, increasing Mach number tends to decrease both desirable and adverse effects of the slats.

Optimum Slat-Opening Angle of Attack

The optimum slat-opening angle of attack is dependent upon the angle at which the aerodynamic characteristics of the airplane would be improved. To obtain this optimum angle may require that the slats be moved progressively further open with increasing angle of attack until full extension is reached or that the slats be fully extended immediately with no further change in angle of attack. In order to determine the angle at which opening should start and the rate of progression, the lift-drag curves of the airplane for various increments of slat position from closed to full open are needed. The envelope of the family of L/D curves specifies the angle at which each partially open slat position is to be reached. Since no data are available on the effect of partially open slat positions on the model aerodynamic characteristics, however, the following discussion is based on the data obtained with the slats in the full-open and almost-closed positions.

A plot of the angles of attack at which the slats would start to open and the angles at which full extension would occur, based on the zero moment coefficient for the slats, is shown in figure 13. The data

of figure 13 neglect the effect of friction and gravity which would retard opening and closing. Included is a curve of the angles of attack for which no difference of L/D occurs with change of slat position. At angles of attack above this curve L/D is improved by opening the slats and at lower angles there is a loss in L/D. The angle of attack at which the unstable pitching-moment break occurs for the slats-closed configuration is also shown in figure 13. The pitch-up usually occurred at higher angles of attack than the angles for a gain in L/D. For maximum aerodynamic benefit, the slats should be opened at angles of attack coinciding as nearly as possible with the L/D boundary, but before pitch-up occurs. Although the slats reach the open position at nearly the optimum angle of attack, they begin opening several degrees too soon with a resulting loss of L/D of the order indicated in figure 12. Ideally, from the aerodynamic standpoint, the most efficient slat-opening and slat-closing characteristics appear to be immediate extension or retraction of the slat at the desired angle of attack; that is, no lag between the open and closed positions. This movement of the slat would occur at the angles at which the slats may be opened or closed with small effects on the aerodynamic and trim characteristics.

Effect of Slat-Rotation-Point Location On Slat-Opening Angle of Attack

A simple method of operation of movable slats consists of using circular-arc mounting tracks within the wing, the centers of which form an imaginary axis below the wing about which the slats pivot. Although opening paths other than a circular arc may be used to advantage, this particular configuration is considered because of its simplicity. A more complete treatment of the aspects of designs of mechanisms adaptable for automatic slats is found in reference 15.

There are some optimum angles of attack, based on gains in L/D, for instance, at which the slats should start opening and should be fully open. The possibility of matching these optimum angles of attack with the opening and closing angles of the slat depends on the choice of the slat rotation point. The effect of the slat rotation point on the opening and closing characteristics of the slats is evaluated. A field of alternate slat pivot points was assumed and the angles of attack for which zero moment would occur over this field were calculated for the two slat positions. By changing the slat rotation point, the open attitude of the slat would also be changed; therefore, a geometrical relation of gap and deflection was chosen in which the radial extension r was held constant (fig. 14).

The assumption was made that the forces and moments varied linearly from the closed- to the open-slat positions. The method used to calculate

the opening characteristics of the slats for other rotation points is found in the appendix. The results of this study are presented in figure 15 where the zero-moment conditions for the entire slats are plotted as surfaces against slat-rotation-point location X/c, Y/c and angle of attack α. Increasing X/c, that is, moving the pivot point rearward, tends to increase the angle of attack at which zero moment occurs, until a limit is reached beyond which no angle of attack will satisfy the zero-moment condition. The slats will not open in this region. There is, however, no limitation in the Y/c direction, because an infinite Y/c represents a translation of the slats with no change in deflection angle.

For immediate rotation of the slats to the open positions, the zero moment for the open and closed slats must exist at the same angle of attack; that is, the two surfaces must intersect. Although some reduction of the angle-of-attack difference between the two surfaces exists as Y/c is increased (fig. 15(a), (b)), in general, the location of the rotation point has small effect on the lag angle. Within the limits of this discussion, therefore, the choice of slat-rotation-point location for Mach numbers 0.60 and 0.85 would mainly affect the angle of attack at which the slats open and is not critical with respect to lag angle. The zero-moment surfaces for the two subsonic Mach numbers show characteristics very similar to each other, but at Mach number 1.00 (fig. 15(c)), the zero moment for slats open fails to exhibit the sudden abrupt rise in angle of attack with increasing horizontal rotation-point location found at the subsonic Mach numbers, and a zero lag angle condition does occur. The angle of attack at which the zero lag condition can be attained is about a degree higher than the optimum opening angle (fig. 13) for the Y/c values considered, but the trend is for the zero-lag condition to decrease in angle of attack with increase of Y/c.

CONCLUSIONS

The results of the investigation of the aerodynamic loading and opening characteristics of leading-edge slats on a 45° sweptback wing at transonic speeds have indicated the following conclusions:

1. Mach number usually had little effect on the maximum values of slat force and moment coefficients obtained for all slat configurations investigated.

2. The spanwise-load distribution was such that the loads on the individual slat segments increased toward the tip for moderate angles of attack and decreased toward the tip for high angles of attack.

3. Slat chord-force coefficients which generally acted in the thrust direction varied approximately linearly with normal-force coefficient to the normal force value at which separation was expected to exist for all slat configurations through the Mach number range investigated.

4. Extension of the slats caused the slat force and moment curves to shift to higher angles of attack with only slight changes in the slope of the curves.

5. The rotation point for aerodynamically operated slats extending along a circular-arc path can be located to cause the slats to be open at the angle of attack at which increased airplane performance first occurs.

6. Some change in opening and closing lag may be obtained by choosing alternate slat-rotation-point locations; however, the amount of lag for a given location varies with Mach number.

Langley Aeronautical Laboratory,
National Advisory Committee for Aeronautics,
Langley Field, Va., September 11, 1953.

APPENDIX

DERIVATION OF EQUATION FOR DETERMINING THE ANGLE OF ATTACK FOR SLAT ZERO PITCHING MOMENT ABOUT ANY ROTATION POINT

The development of the equation for determining the opening and closing characteristics of any slat which extends and retracts along a circular-arc path is based on the relation of the moment of the resultant-slat-force vector about any rotation point. A sketch showing the geometric relations is presented here

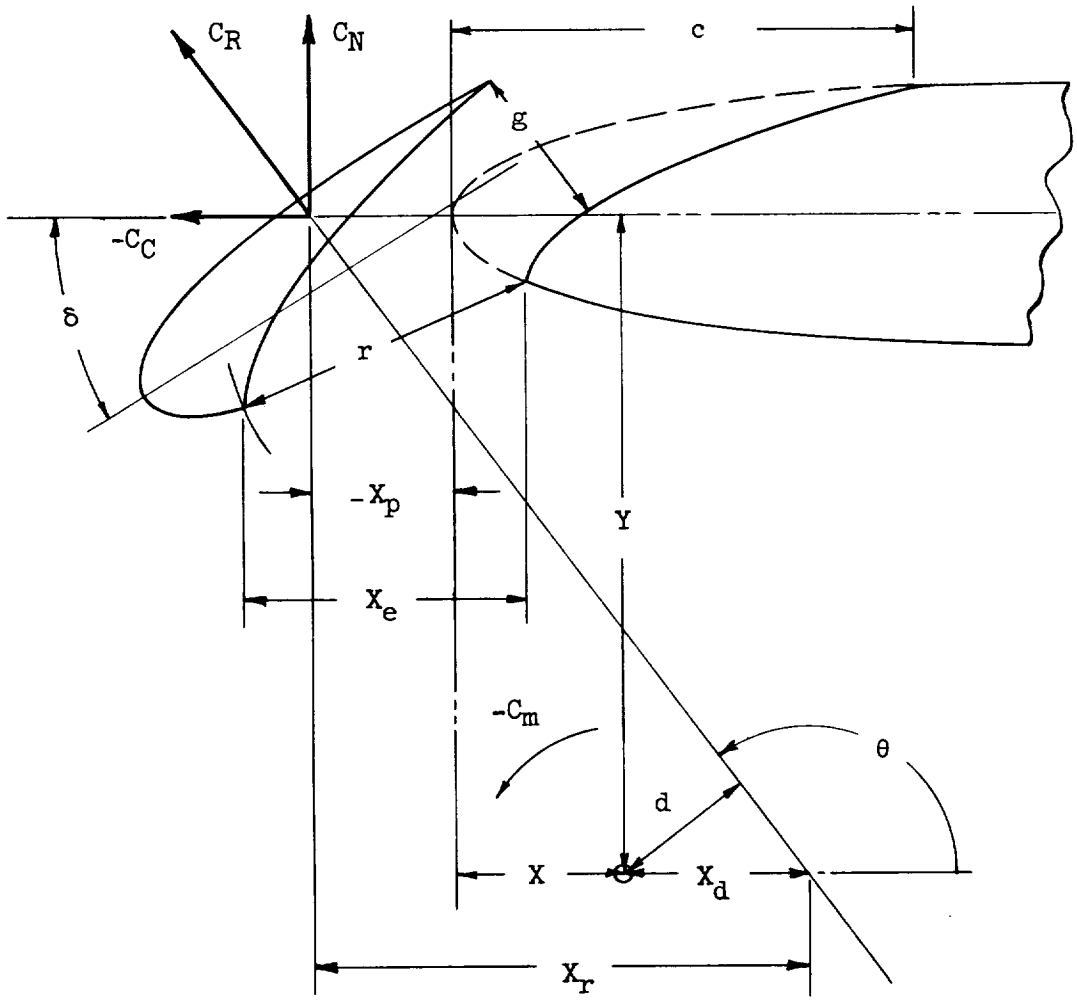

where X_p is the center of pressure of the slat measured parallel to the wing chord line from the leading edge of the wing to the intersection of the resultant-force vector with the wing chord line. Note that X_p as defined here differs from x_p/c given in the section entitled "SYMBOLS" and used in figure 11.

$$X_r = Y \cot \theta$$

$$X_d = d \csc \theta$$

where

$$\cot \theta = \frac{C_C}{C_N} \text{ and } \csc \theta = \frac{C_R}{C_N}$$

$$d = \frac{C_m}{C_R}$$

(Note that for the case shown C_C, C_m, X_p, and $\cot \theta$ are negative.)

$$X_p = X + X_d - X_r$$

or

$$X_p = X - \frac{C_m}{C_N} + Y \cot \theta$$

The slats will start to open or close when the moment coefficient is zero. Therefore

$$X_p - X = Y \cot \theta \qquad (1)$$

X_p and $\cot \theta$ are both functions of the angle of attack for constant X,Y so that equation (1) could be solved for the zero-moment angle of attack. The variation in X_p and $\cot \theta$ with angle of attack is known only for the test slat rotation point X_o, Y_o in the extended and almost-closed positions.

Equation (1) can be written in differential form as follows:

$$\frac{\partial X_p}{\partial X} dX + \frac{\partial X_p}{\partial Y} dY - dX = \cot \theta \, dY + Y\left(\frac{\partial \cot \theta}{\partial X} dX + \frac{\partial \cot \theta}{\partial Y} dY\right) \quad (2)$$

By varying X and Y from the original position X_o, Y_o the opened-slat attitude must necessarily change if the slats are to follow a circular-arc path. (Varying X and Y does not affect the slat in the closed position.) The attitude of the slat is fixed by specifying the extension, gap, and deflection so that the orientation X_e, g, δ will be a function of X,Y.

If the radial extension r is held constant (in order to give practical slat arrangements) and the change in r cos δ is small for the X,Y values considered, the slat extension X_e will be nearly constant. Specifically, the variation of slat gap and deflection with X and Y will be as shown in figure 14. Equation (2) can now be rewritten as follows:

$$\frac{\partial X_p}{\partial \delta} \frac{\partial \delta}{\partial X} dX + \frac{\partial X_p}{\partial g} \frac{\partial g}{\partial X} dX + \frac{\partial X_p}{\partial \delta} \frac{\partial \delta}{\partial Y} dY + \frac{\partial X_p}{\partial g} \frac{\partial g}{\partial Y} dY - dX =$$

$$\cot \theta \, dY + Y\left(\frac{\partial \cot \theta}{\partial \delta} \frac{\partial \delta}{\partial X} dX + \frac{\partial \cot \theta}{\partial g} \frac{\partial g}{\partial X} dX + \right.$$

$$\left. \frac{\partial \cot \theta}{\partial \delta} \frac{\partial \delta}{\partial Y} dY + \frac{\partial \cot \theta}{\partial g} \frac{\partial g}{\partial Y} dY\right) \quad (3)$$

and rewriting equation (3) in terms of the total derivatives of gap and deflection gives

$$\frac{\partial X_p}{\partial \delta} d\delta + \frac{\partial X_p}{\partial g} dg - dX = \cot \theta \, dY + Y\left(\frac{\partial \cot \theta}{\partial \delta} d\delta + \frac{\partial \cot \theta}{\partial g} dg\right) \quad (4)$$

An approximate evaluation of the partial derivatives $\frac{\partial X_p}{\partial \delta}$, $\frac{\partial X_p}{\partial g}$, $\frac{\partial \cot \theta}{\partial \delta}$, $\frac{\partial \cot \theta}{\partial g}$ for a constant angle of attack can be made by assuming, first, that the derivatives are constant and, second, that the partials can be simply determined from the open- and closed-slat data. The term $\frac{\partial X_p}{\partial g}$ was neglected because a study of unpublished pressure distributions of slats showed, in general, that the effect of gap on center of pressure was small. The remaining derivatives were interpreted from the open and closed variation of X_p and θ with angle of attack as shown

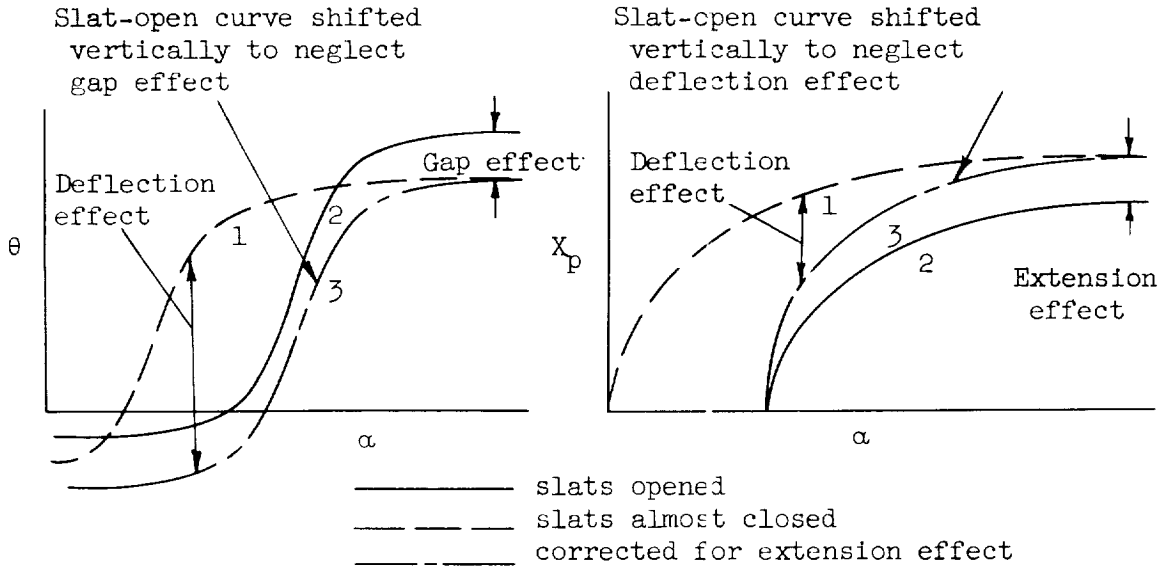

The effect of δ on X_p was determined by assuming that, in translating the slat forward, the slat center of pressure would move forward approximately the same amount as the slat itself. At high angles of attack the effect of deflection would be small since once separation occurred on the slats proper, increasing δ or α would not appreciably change X_p. Therefore, the difference between the curves for the slats almost closed and open at high angles of attack was chosen to determine the extension effect (see graphs above). By adding this constant difference to the values of X_p for the open slats at all angles of attack, a new curve, corrected for effect of extension, was formed. The difference between this corrected curve and the curve of X_p for the almost-closed slats at any angle of attack was considered as the effect of δ alone on X_p.

The effect of δ and g on θ can also be determined by similar considerations. In this case, the effect of δ on θ disappears at high angles of attack and the difference between the open and almost-closed curves is attributed to gap effect alone. A change in gap will change the underslat pressures for practical slat attitudes, and in general the effect of the gap on the change of pressure with α will be assumed small. Therefore the effect of the underslat pressure on θ (or of gap on θ) will be assumed constant with α so that at the high angles of attack the effect of gap can be evaluated for the two slat positions. Subtracting this constant value from the slat-open curve gives a curve corrected for gap, and the difference between this curve and the curve for the slat almost closed gives the effect of δ on θ. From the above interpretations of the effect of δ and g on θ and X_p, the partial derivations of equation (4) can be evaluated

$$\frac{\partial X_p}{\partial \delta} = \frac{X_{p3} - X_{p1}}{\delta_3 - \delta_1}$$

$$\frac{\partial \cot \theta}{\partial \delta} = \frac{\cot \theta_3 - \cot \theta_1}{\delta_3 - \delta_1}$$

$$\frac{\partial \cot \theta}{\partial g} = \frac{\cot \theta_3 - \cot \theta_2}{g_3 - g_2}$$

where subscripts 1 and 2 indicate test values for the slat almost-closed and open positions, respectively, and subscript 3 indicates the adjusted open-slat data.

Inasmuch as the derivatives are linear for constant angles of attack, equation (4) can be integrated to give the total change from the initial point.

Adding equation (1), evaluated at the initial conditions, to the integrated equation (4) gives

$$X_{p_o} + \frac{\partial X_p}{\partial \delta}\left(\delta - \delta_o\right) - X = Y\left[\cot \theta_o + \frac{\partial \cot \theta}{\partial \delta}\left(\delta - \delta_o\right) + \frac{\partial \cot \theta}{\partial g}\left(g - g_o\right)\right]$$

which can be solved graphically for α at various values of X and Y to yield a zero-moment surface.

The closed-slat-position zero-moment surface is readily computed because $X_{p_o} - X = Y \cot \theta_o$ is the equation of a straight line for constant α. Varying α generates the surface of zero moments for the closed slats. The results are shown in figure 15 for three Mach numbers.

REFERENCES

1. Kelly, John A., and Hayter, Nora-Lee F.: Aerodynamic Characteristics of a Leading-Edge Slat on a 35° Swept-Back Wing for Mach Numbers From 0.30 to 0.88. NACA RM A51H23, 1951.

2. Runckel, Jack F., and Steinberg, Seymour: Effects of Leading-Edge Slats on the Aerodynamic Characteristics of a 45° Sweptback Wing-Fuselage Configuration at Mach Numbers of 0.4 to 1.03. NACA RM L53F23, 1953.

3. Queijo, M. J., and Lichtenstein, Jacob H.: The Effects of High-Lift Devices on the Low-Speed Stability Characteristics of a Tapered 37.5° Sweptback Wing of Aspect Ratio 3 in Straight and Rolling Flow. NACA RM L8I03, 1948.

4. Turner, W. N., and Katkov, R. B.: Wind Tunnel Tests of a $\frac{1}{3}$-Scale Semispan Model of the XP-86 Airplane To Determine the Effect of a Revised Slat Position on Stability Slat-Opening Tendencies and Slat Pressures. Rep. No. NA-48-375, North American Aviation Inc., Mar. 24, 1948.

5. Kemp, William B., Jr., and Few, Albert G., Jr.: Pressure Distribution at Low Speed on a $\frac{1}{4}$-Scale Bell X-5 Airplane Model. NACA RM L51I25, 1951.

6. Lipson, Stanley, and Barnett, U. Reed, Jr.: Force and Pressure Investigation at Large Scale of a 49° Sweptback Semispan Wing Having NACA 65A006 Sections and Equipped With Various Slat Arrangements. NACA RM L51K26, 1952.

7. Freeman, F. L.: Low Speed Wind Tunnel Tests of a 0.15-Scale Semi-Span Model of the YF-100A Airplane With Tapered Chord Slats and 275 Gal. Fuel Tanks, To Determine the Stability and Control Characteristics, and Slat Loads. Partial preprint NAAL 235, North American Aviation, Inc.

8. Cahill, Jones F., and Oberndorfer, Gale C.: Pressure Distributions Over a Retracted Leading-Edge Slat on a 40° Sweptback Wing at Mach Numbers up to 0.9. NACA RM L50L04a, 1951.

9. Cahill, Jones F., and Nuber, Robert J.: Aerodynamic Load Measurements Over a Leading-Edge Slat on a 40° Sweptback Wing at Mach Numbers From 0.10 to 0.91. NACA RM L52G18a, 1952.

10. Kennedy, J.: Report on Additional Wind Tunnel Tests of a 0.15-Scale Reflection-Plane Model of the North American, Inglewood, F-100A Airplane. CWT Rep. 292, Southern Calif. Cooperative Wind Tunnel, Mar. 20, 1953.

11. Ward, Vernon G., Whitcomb, Charles F., and Pearson, Merwin D.: Air-Flow and Power Characteristics of the Langley 16-Foot Transonic Tunnel With Slotted Test Section. NACA RM L52E01, 1952.

12. Whitcomb, Charles F., and Osborne, Robert S.: An Experimental Investigation of Boundary Interference on Force and Moment Characteristics of Lifting Models in the Langley 16- and 8-Foot Transonic Tunnels. NACA RM L52L29, 1953.

13. Edwards, George G., and Boltz, Frederick W.: An Analysis of the Forces and Pressure Distribution on a Wing With the Leading Edge Swept Back 37.25°. NACA RM A9K01, 1950.

14. Runckel, Jack F., and Schmeer, James W.: The Aerodynamic Characteristics at Transonic Speeds of a Model With a 45° Sweptback Wing, Including the Effect of Leading-Edge Slats and a Low Horizontal Tail. NACA RM L53J08, 1954.

15. Braun: Studies of the Kinematics of Leading Edge Slats. North American Aviation translation of Untersuchungen von Vorflugelkinematiken. TB-33/41, Mar. 28, 1941. (Translation available from CADO, Wright-Patterson Air Force Base, as ATI32590.)

Beam

Bea

Deflecti

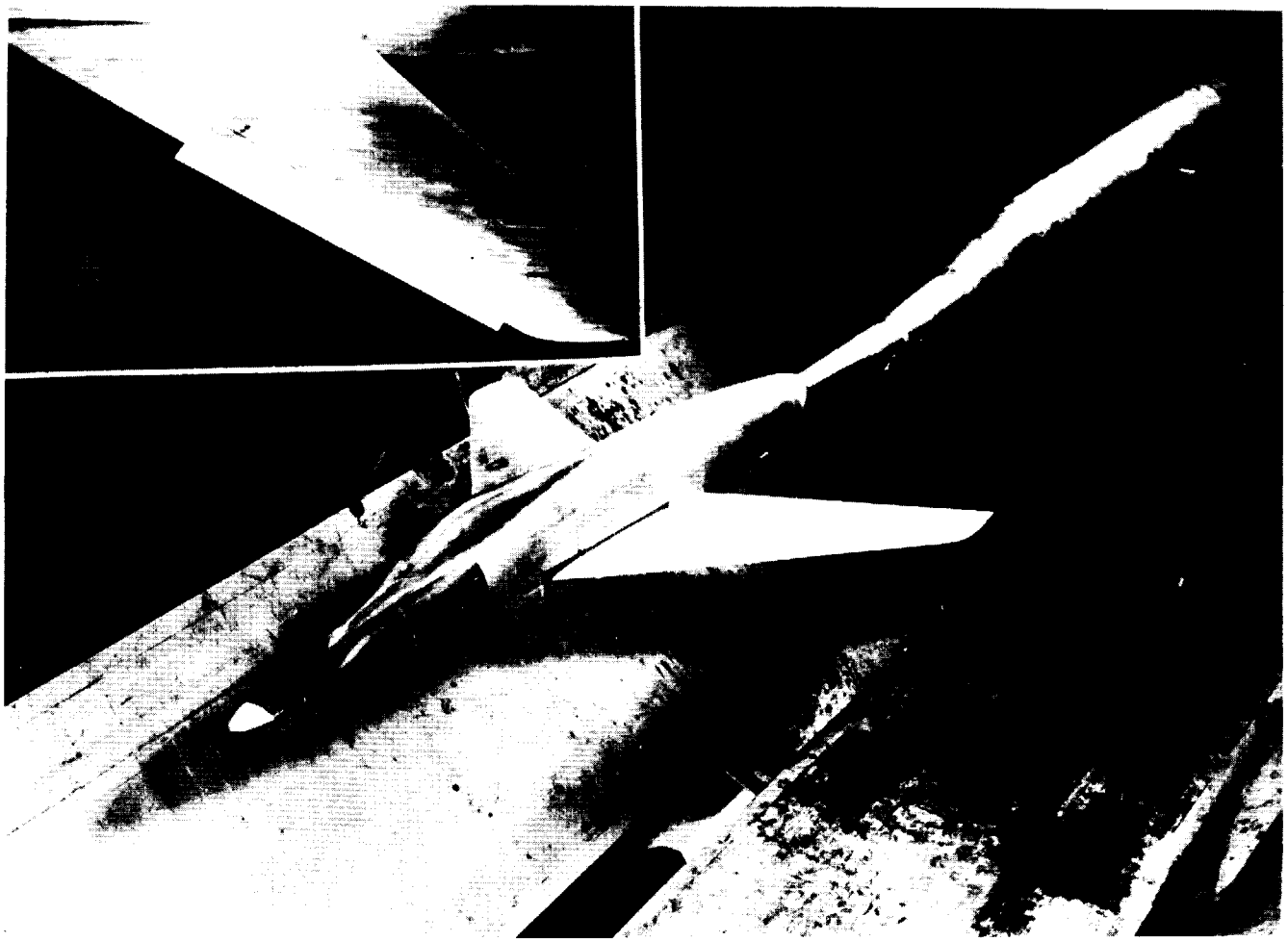

L-79716

Figure 1.- Wing-fuselage model with slats almost closed in the Langley 16-foot transonic tunnel test section. The 46- to 95-percent-semispan slats open are shown in the insert.

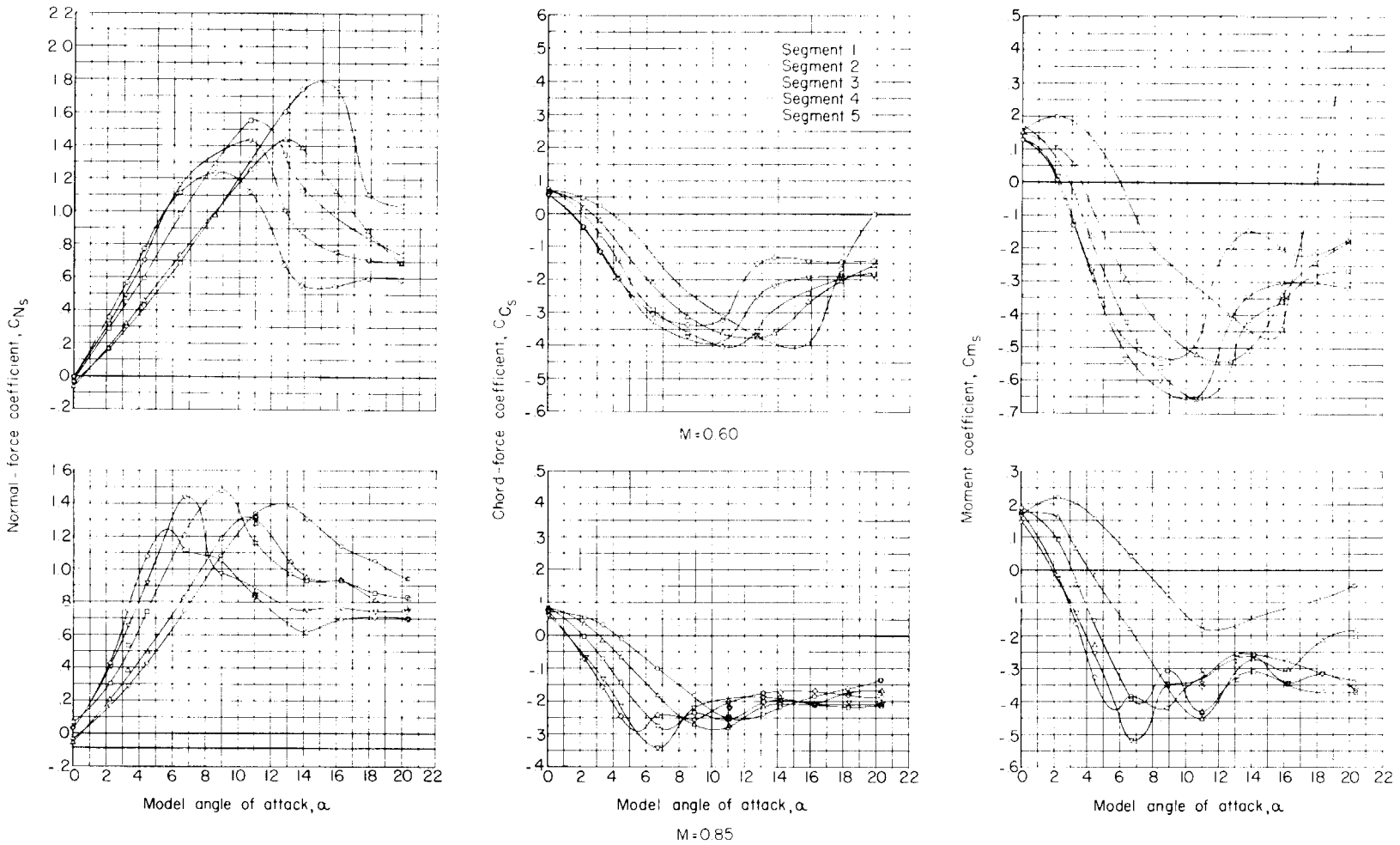

(a) M = 0.60 and M = 0.85.

Figure 4.- Slat-segment coefficients for 25- to 95-percent-semispan slats almost closed.

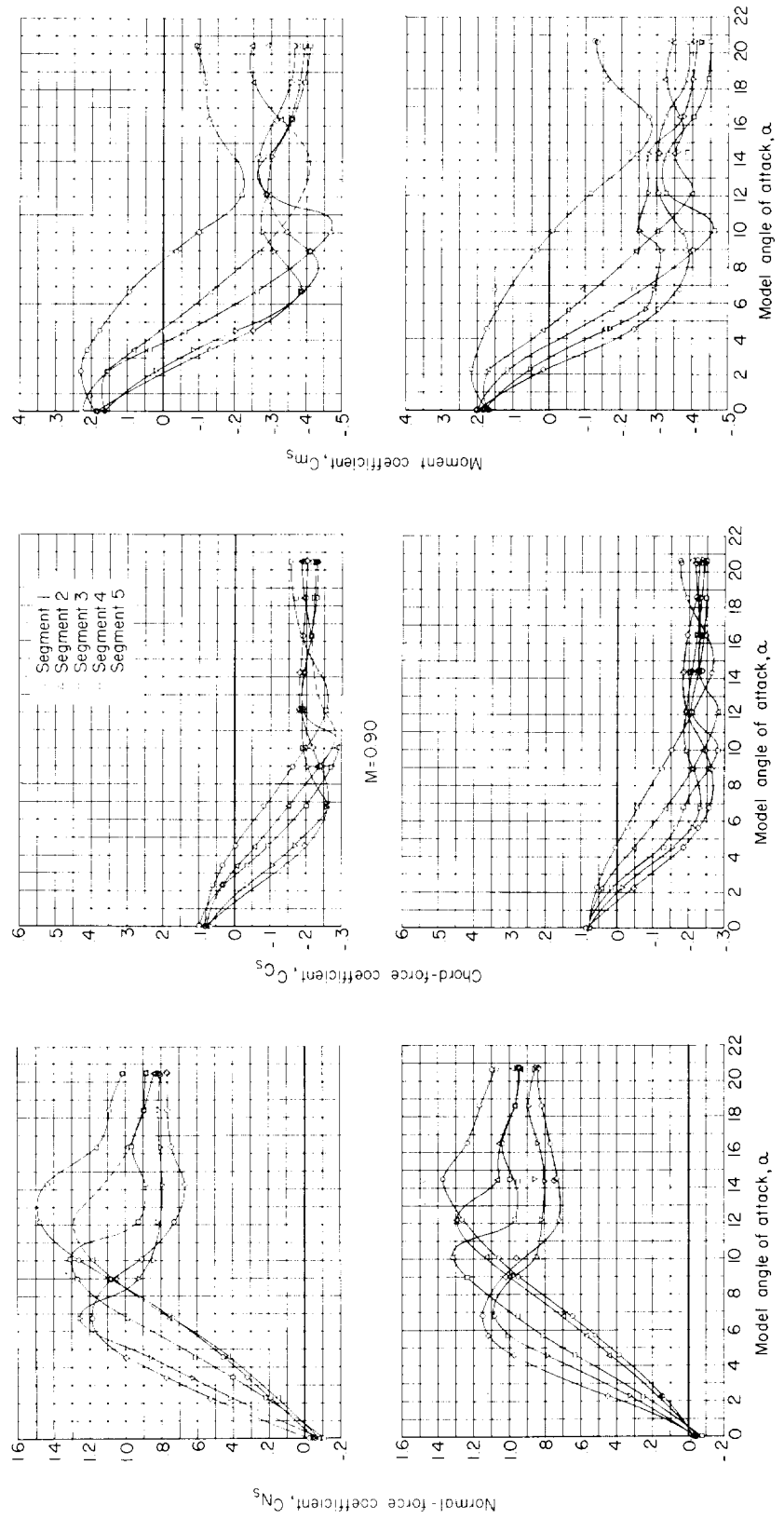

(b) M = 0.90 and M = 0.93.

Figure 4.- Continued.

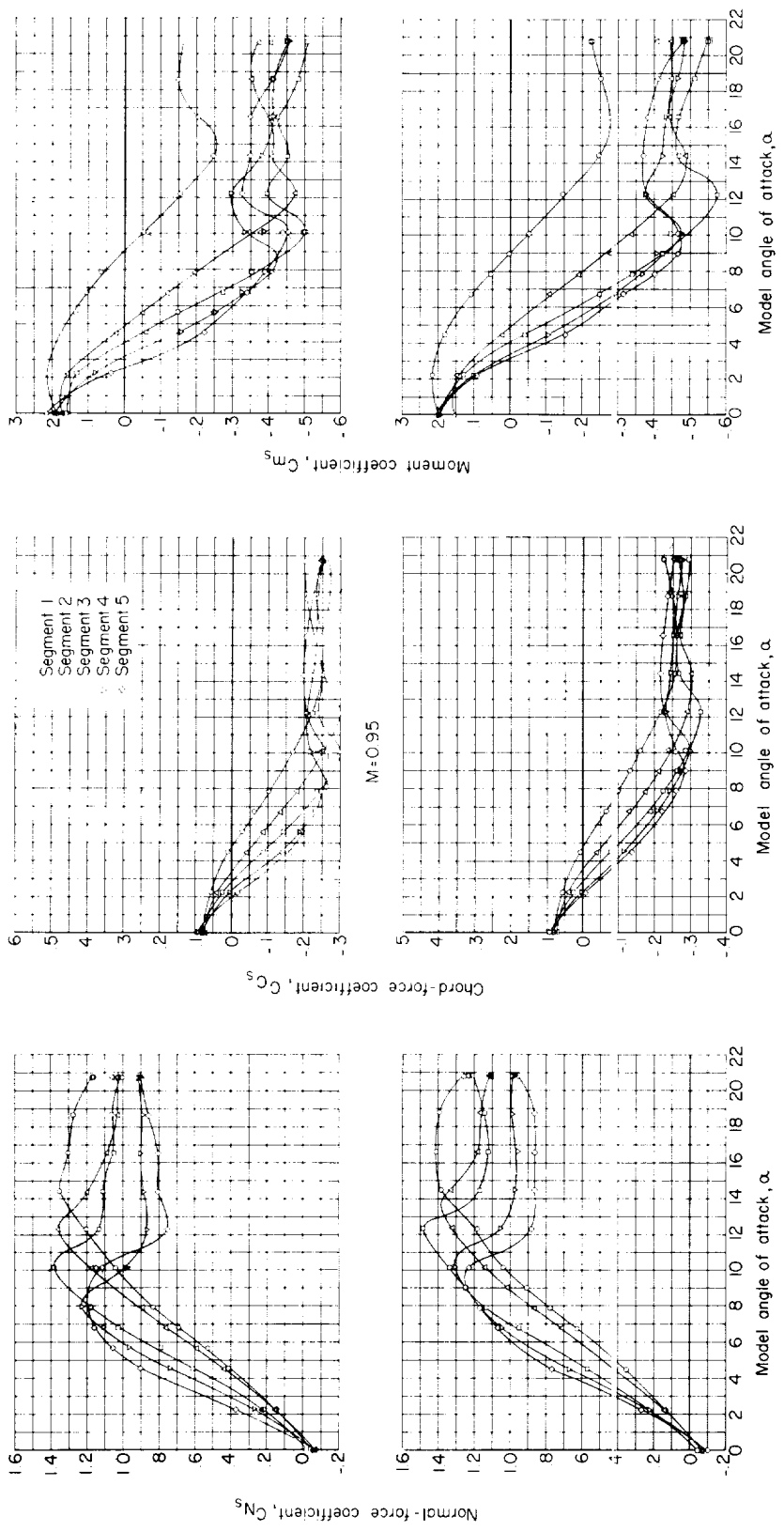

(c) M = 0.95 and M = 0.97.

Figure 4.- Continued.

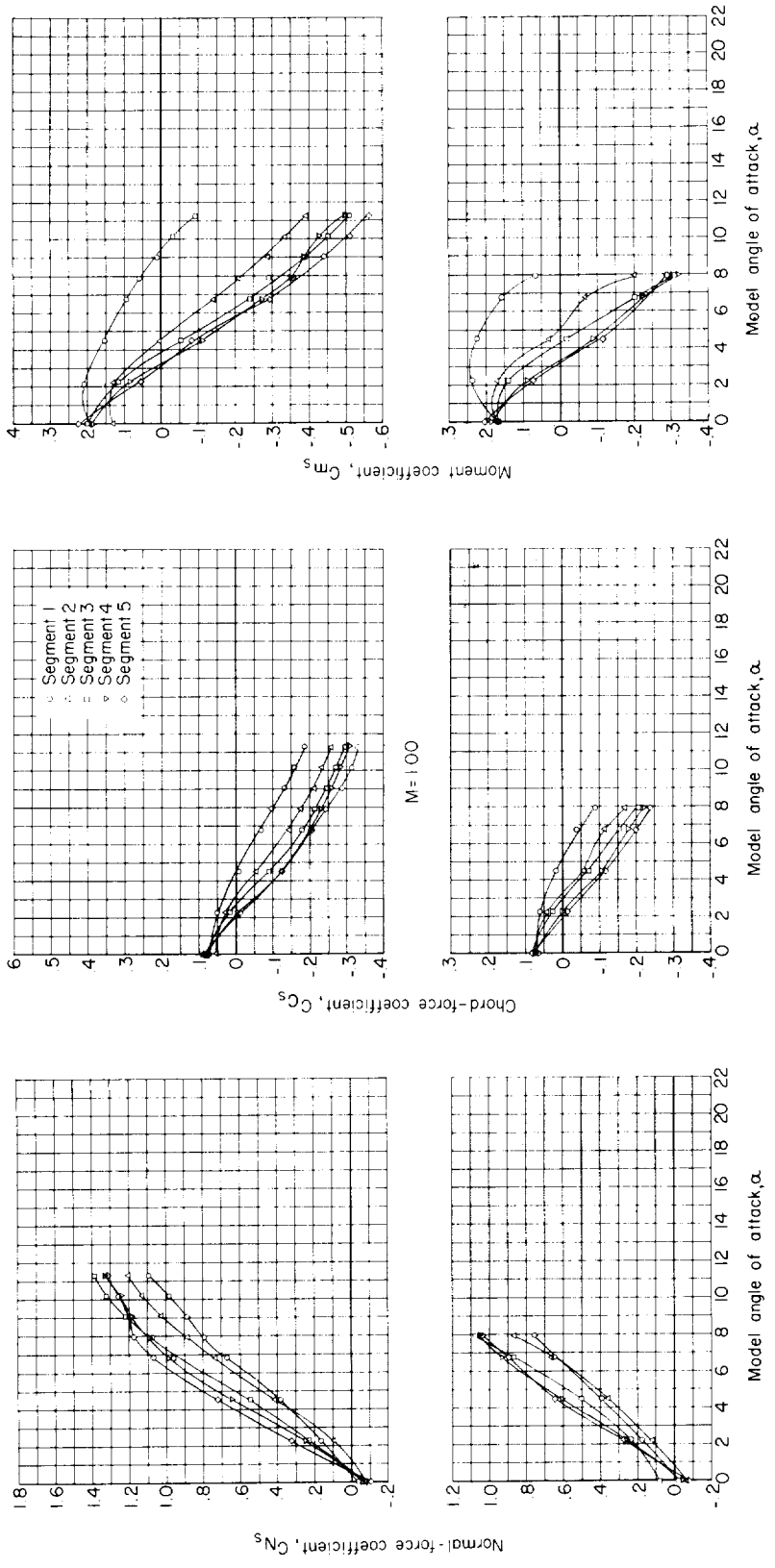

(d) M = 1.00 and M = 1.03.

Figure 4.- Concluded.

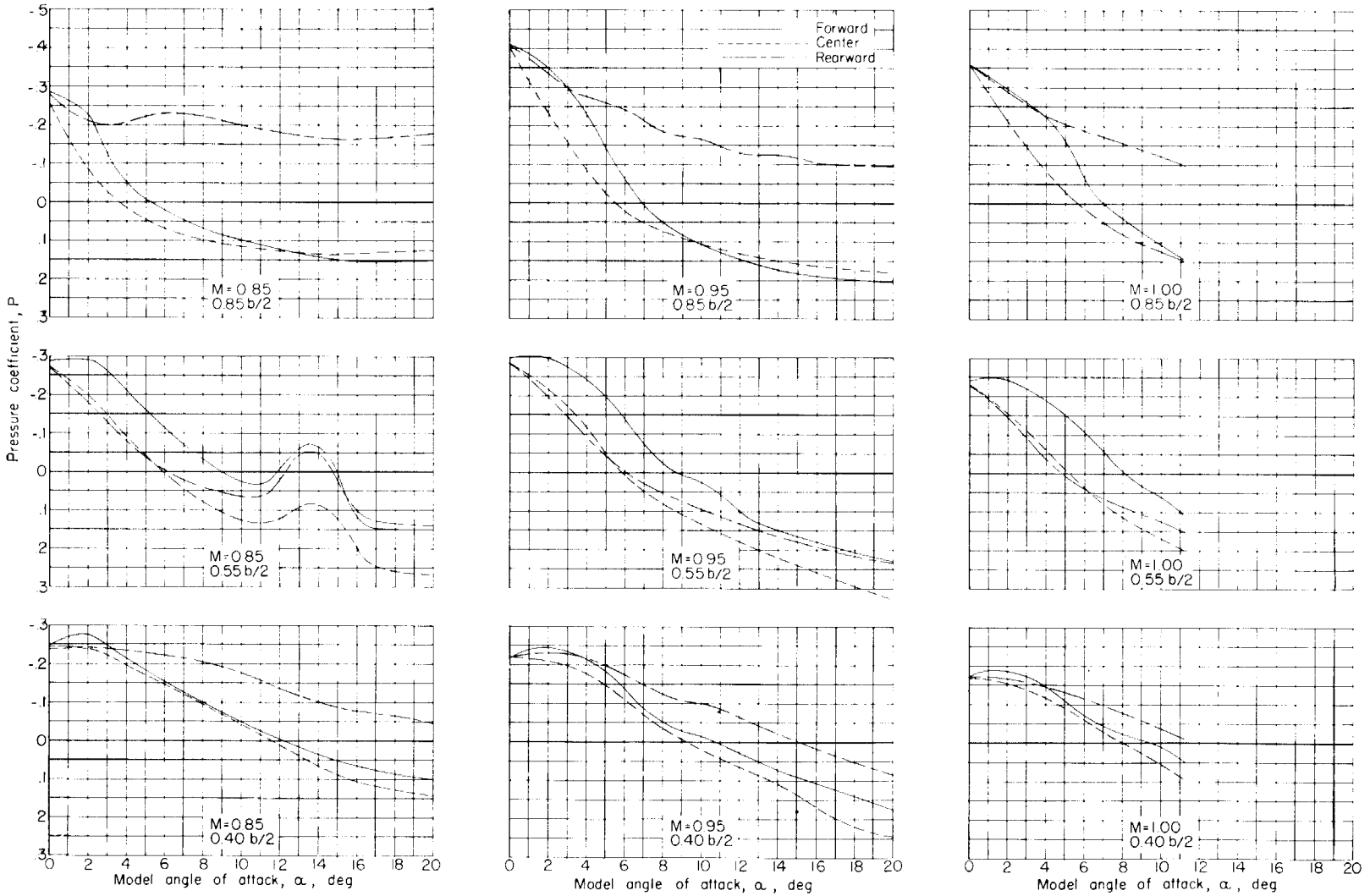

(a) Slats almost closed.

Figure 5.- Underslat pressures for 25- to 95-percent-semispan slats.

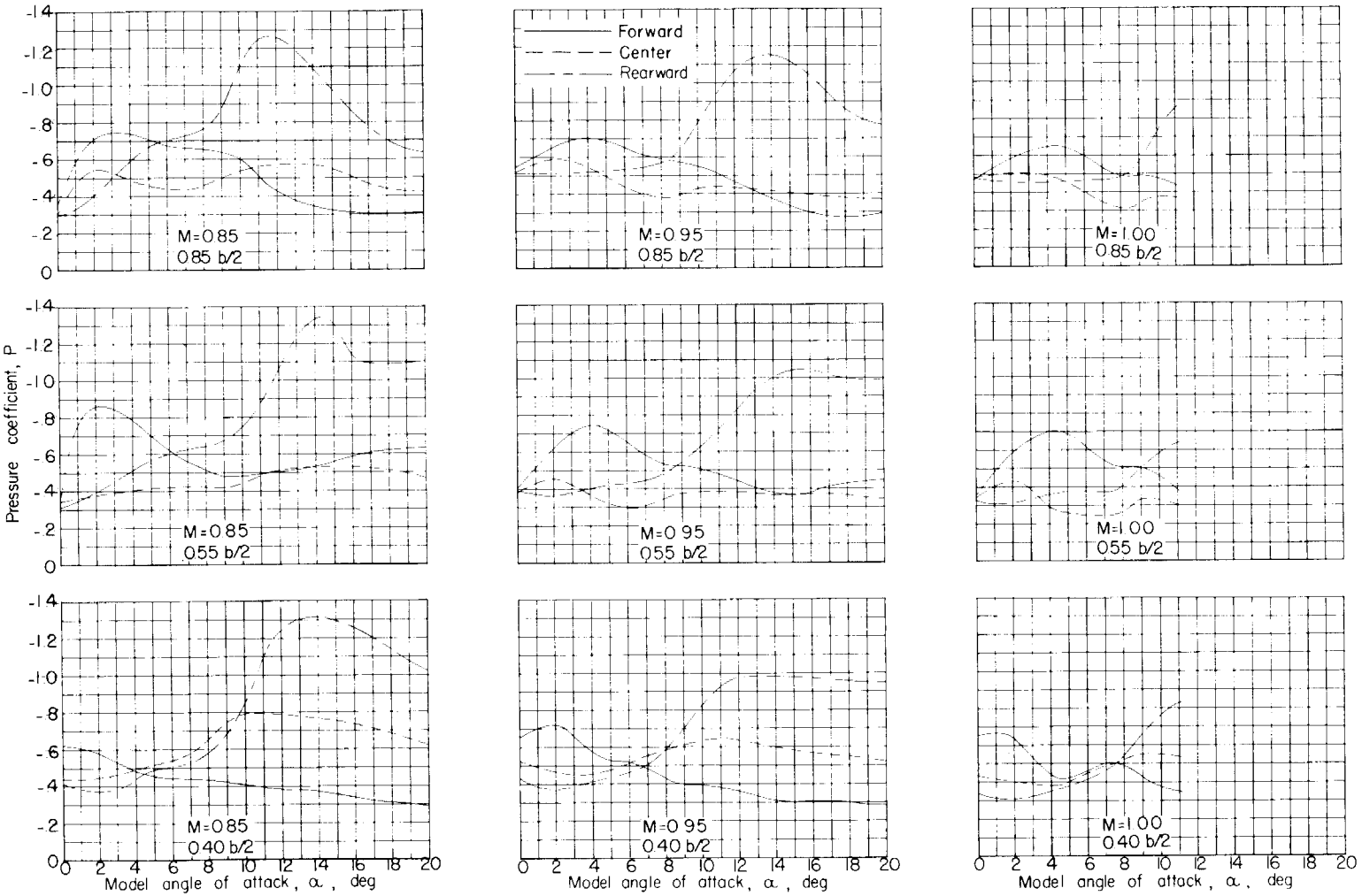

(b) Slats open.

Figure 5.- Concluded.

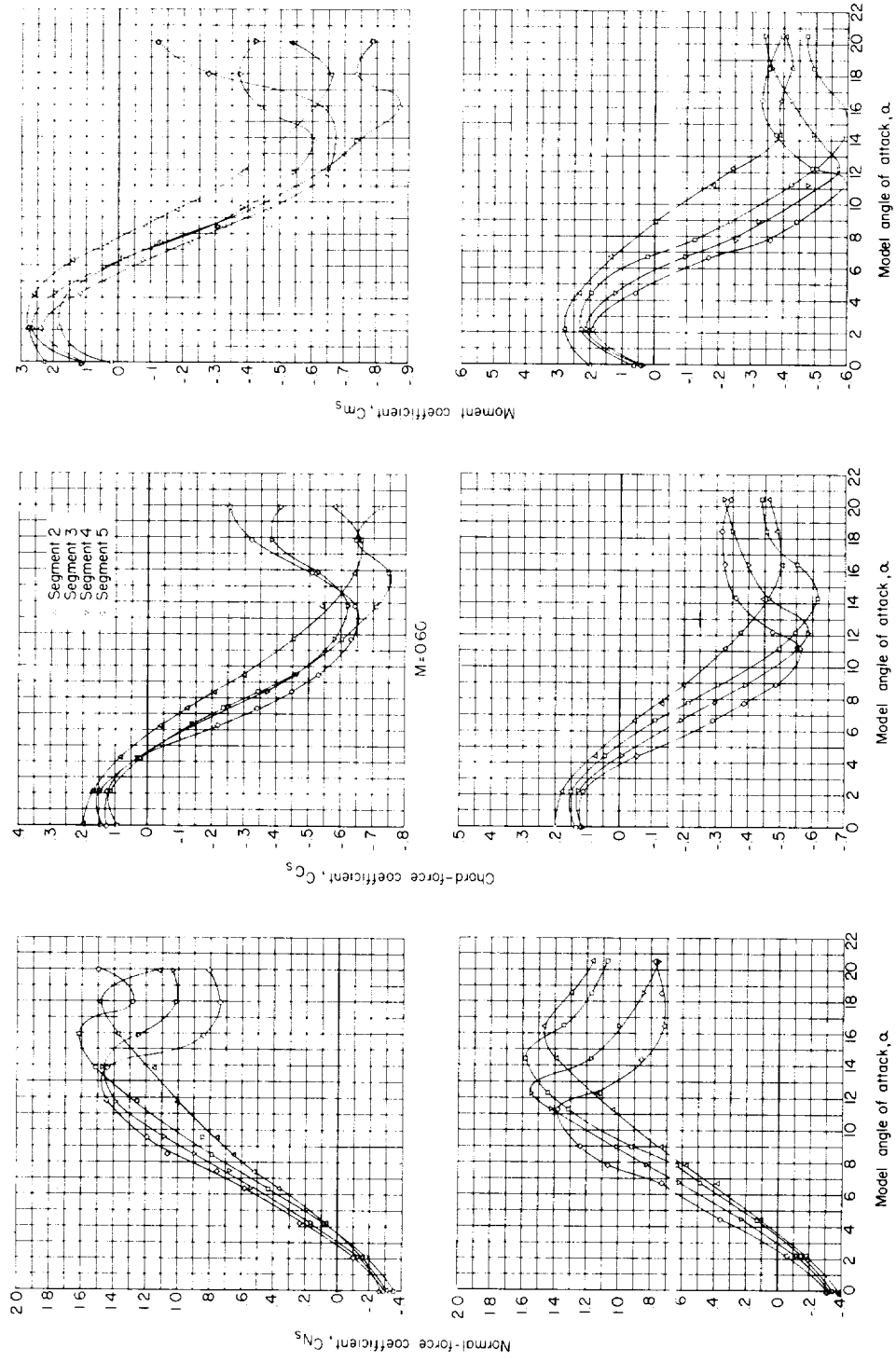

(a) M = 0.60 and M = 0.85.

Figure 6.- Slat-segment coefficients for 35- to 95-percent-semispan slats open.

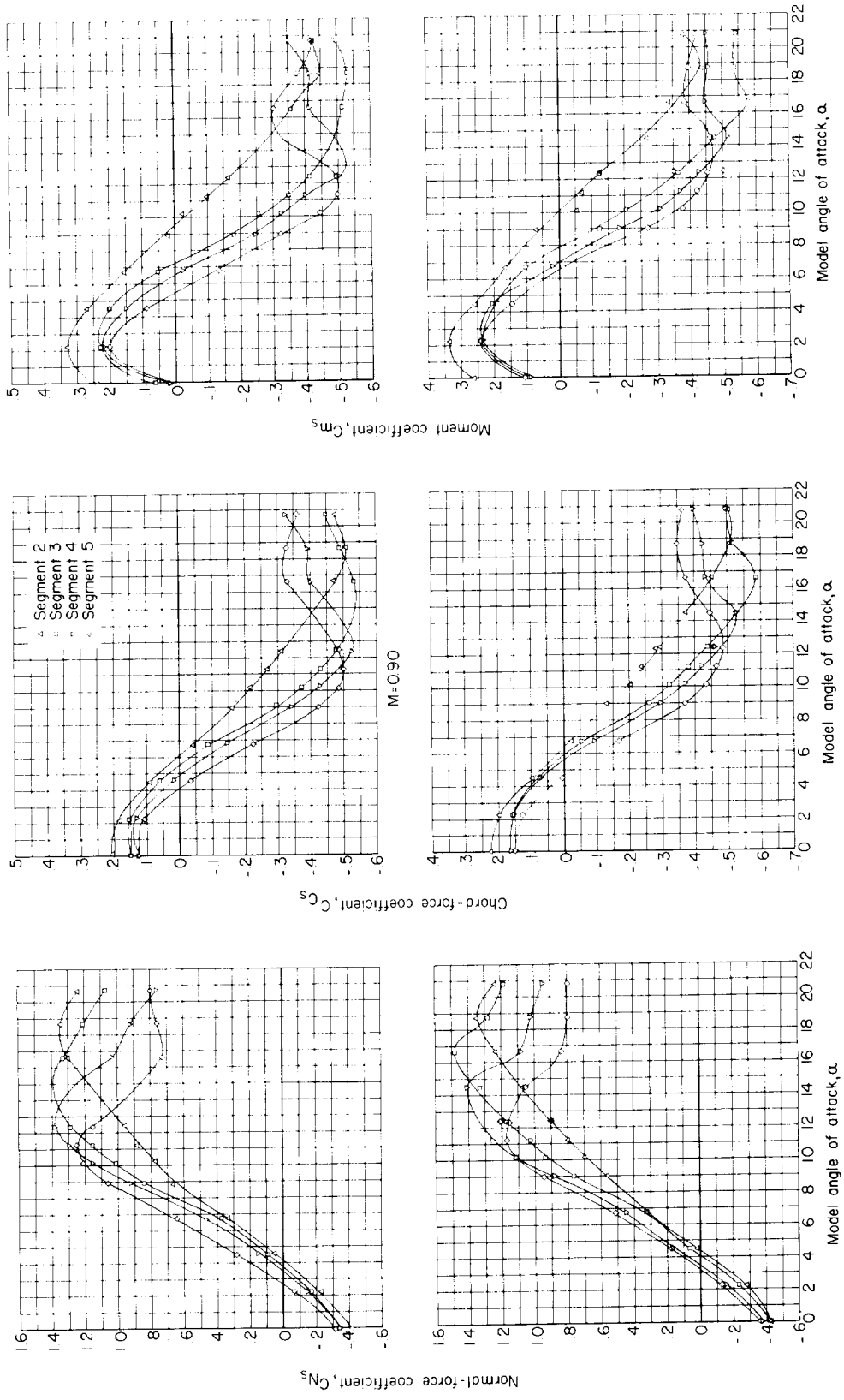

(b) M = 0.90 and M = 0.93.

Figure 6.- Continued.

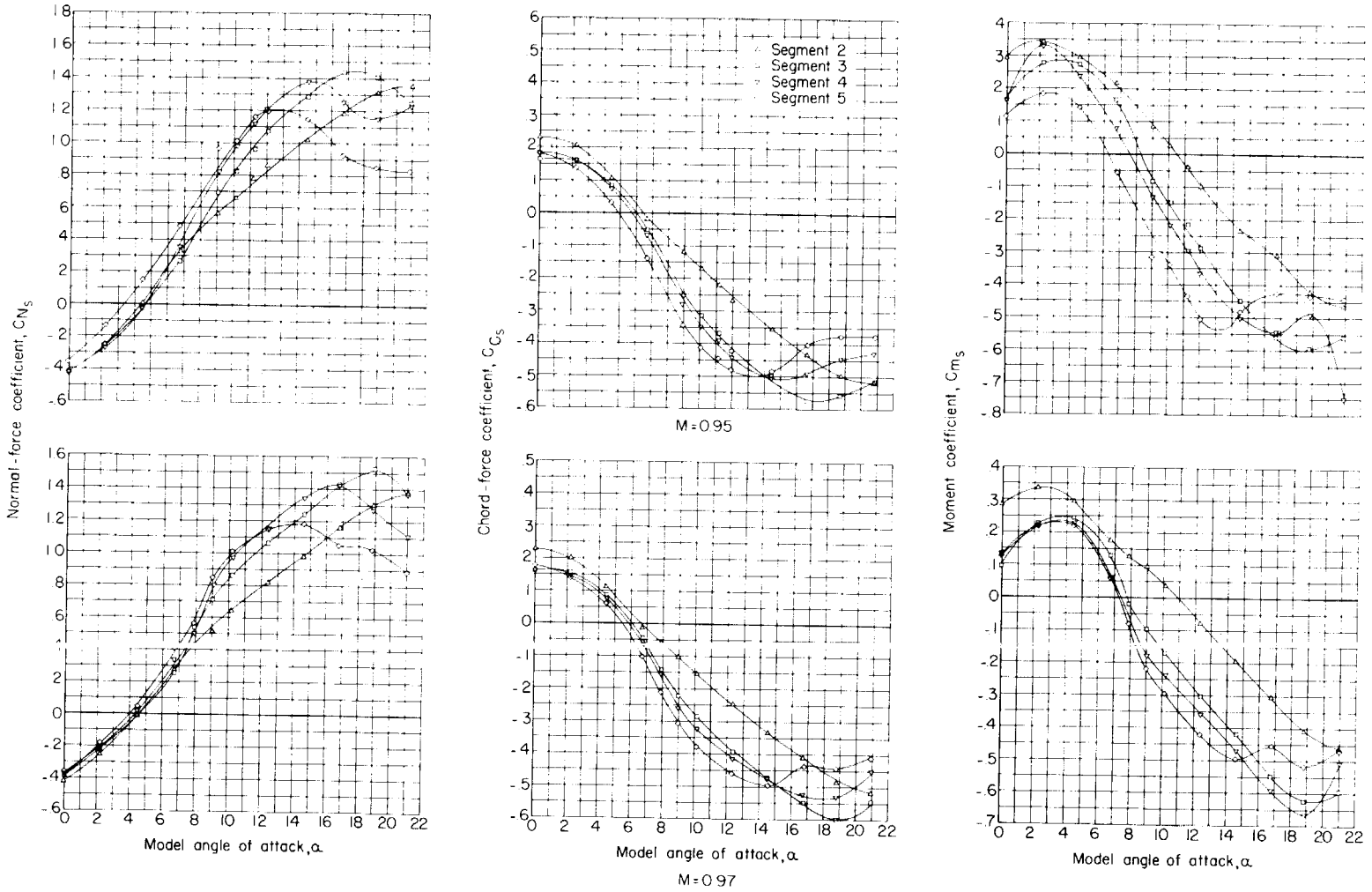

(c) M = 0.95 and M = 0.97.

Figure 6.- Continued.

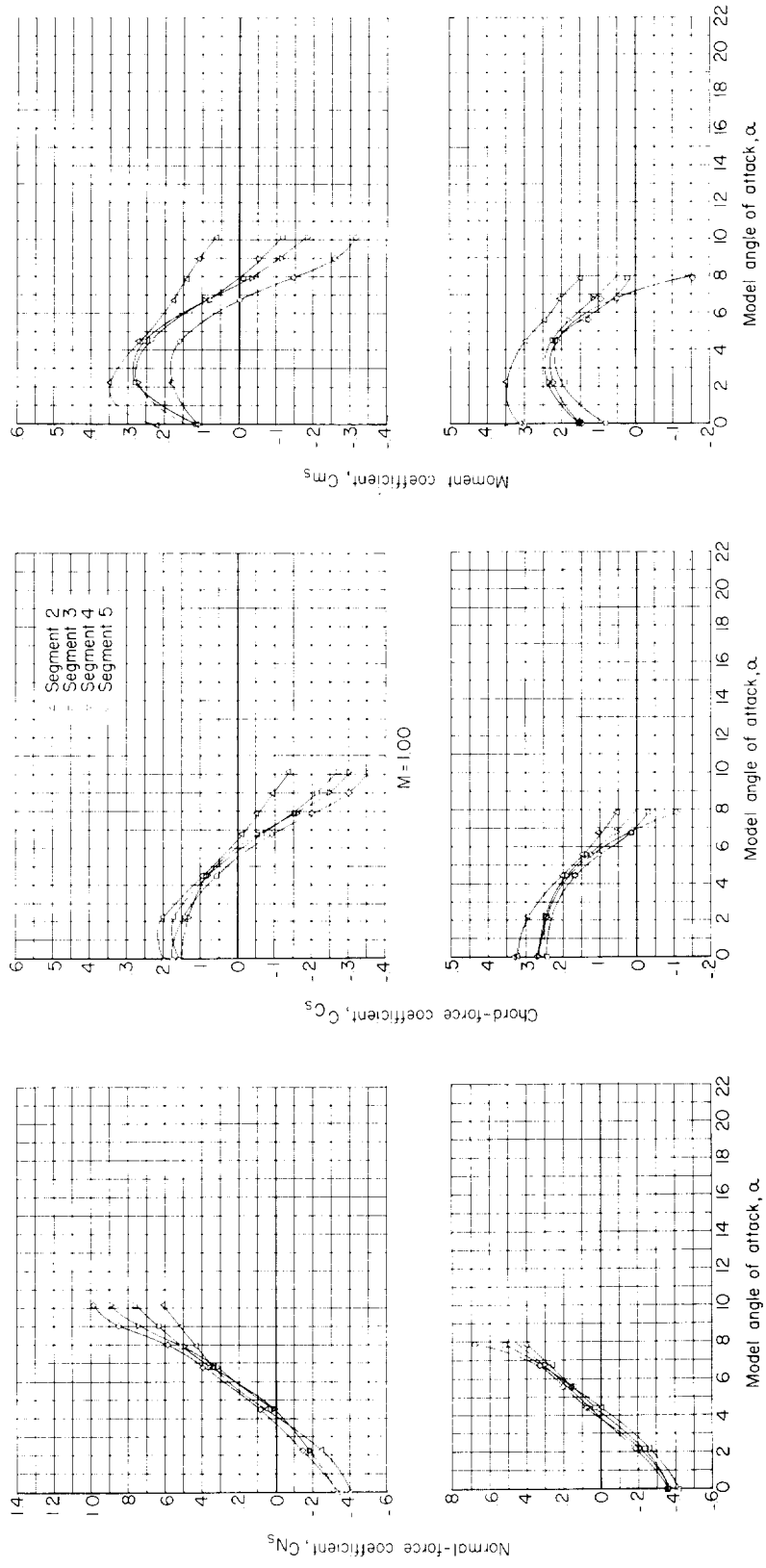

(d) M = 1.00 and M = 1.03.

Figure 6.- Concluded.

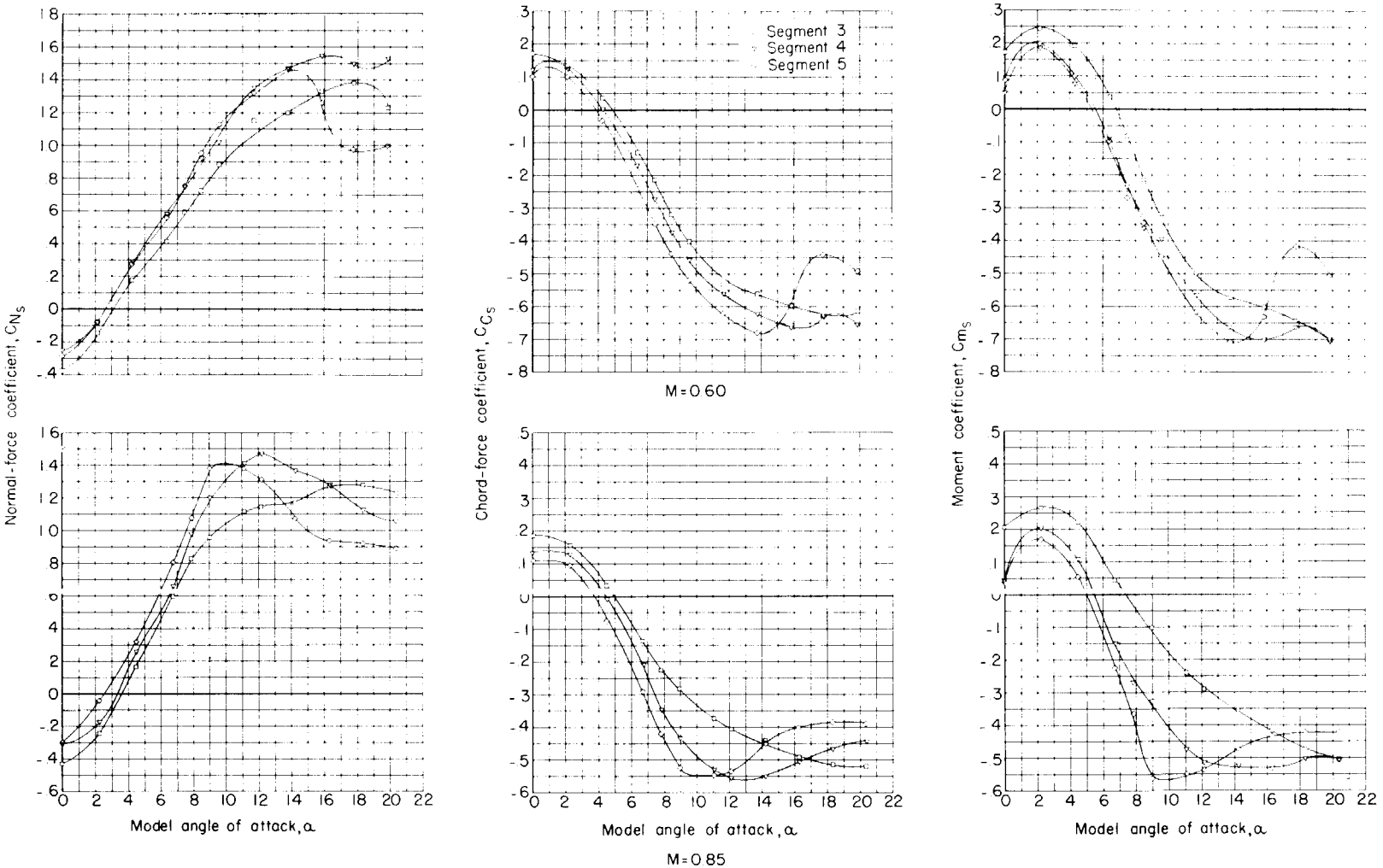

(a) M = 0.60 and M = 0.85.

Figure 7.- Slat-segment coefficients for 46- to 95-percent-semispan slats open.

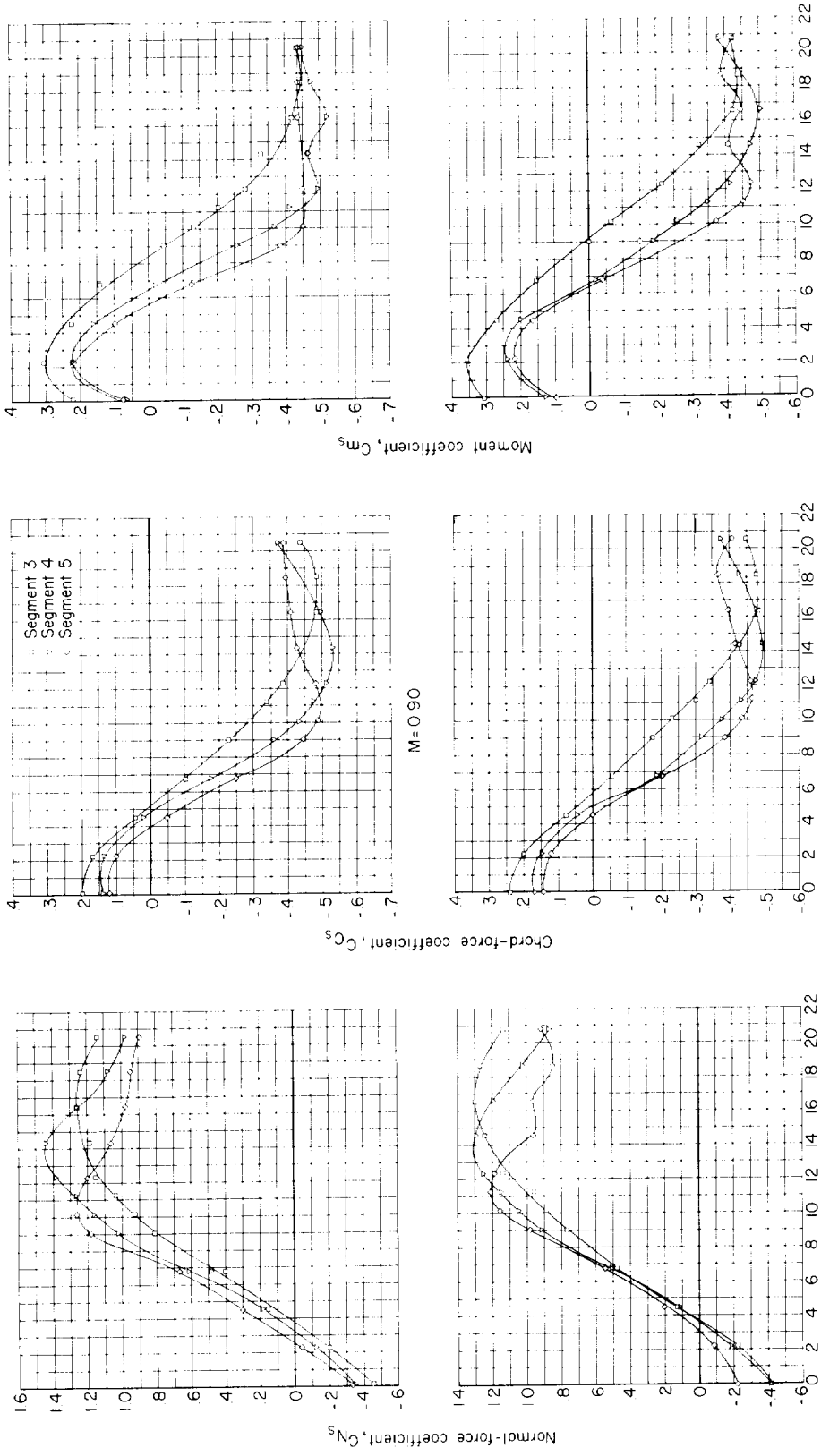

(b) M = 0.90 and M = 0.93.

Figure 7.- Continued.

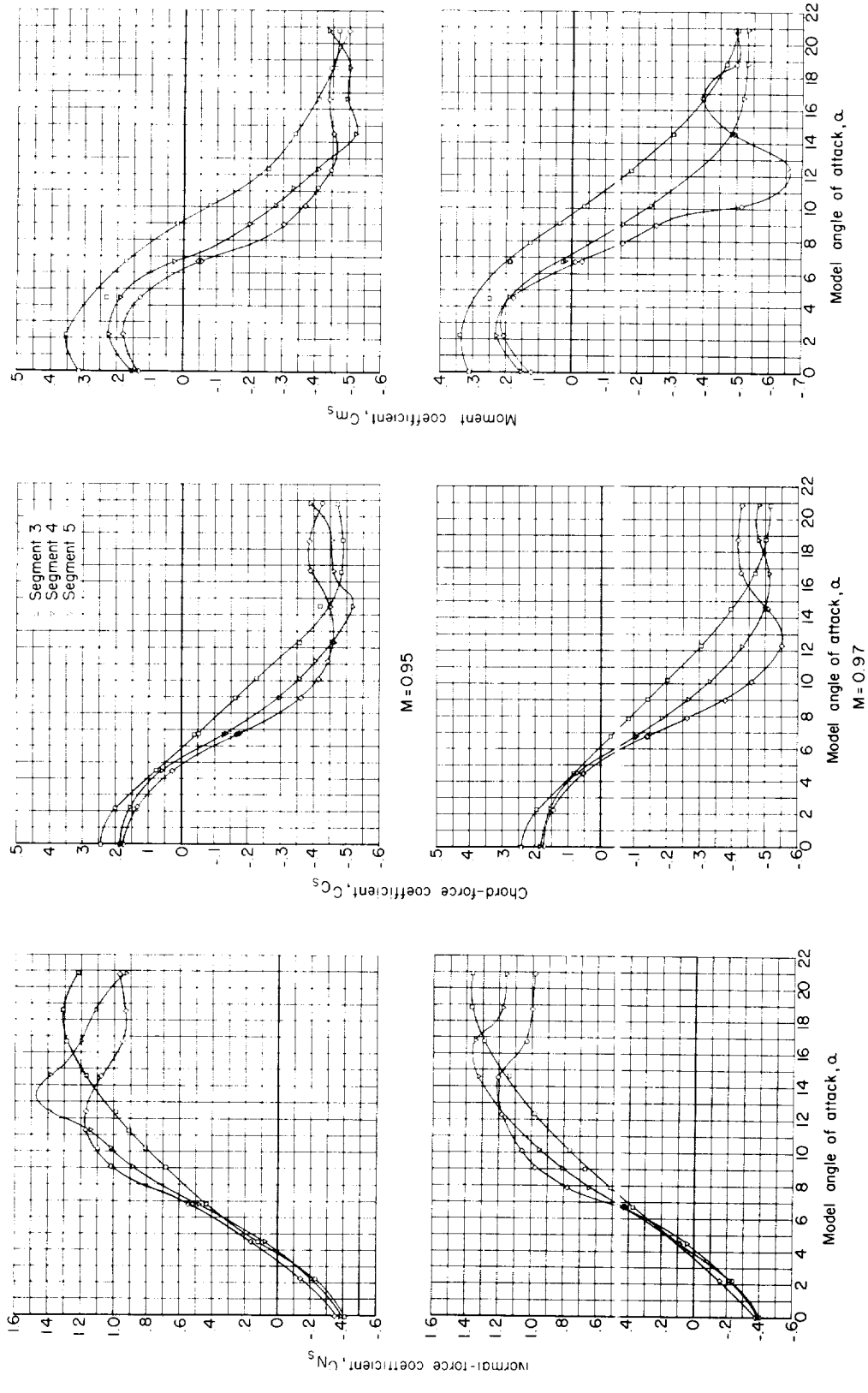

(c) M = 0.95 and M = 0.97.

Figure 7.- Continued.

L-1609

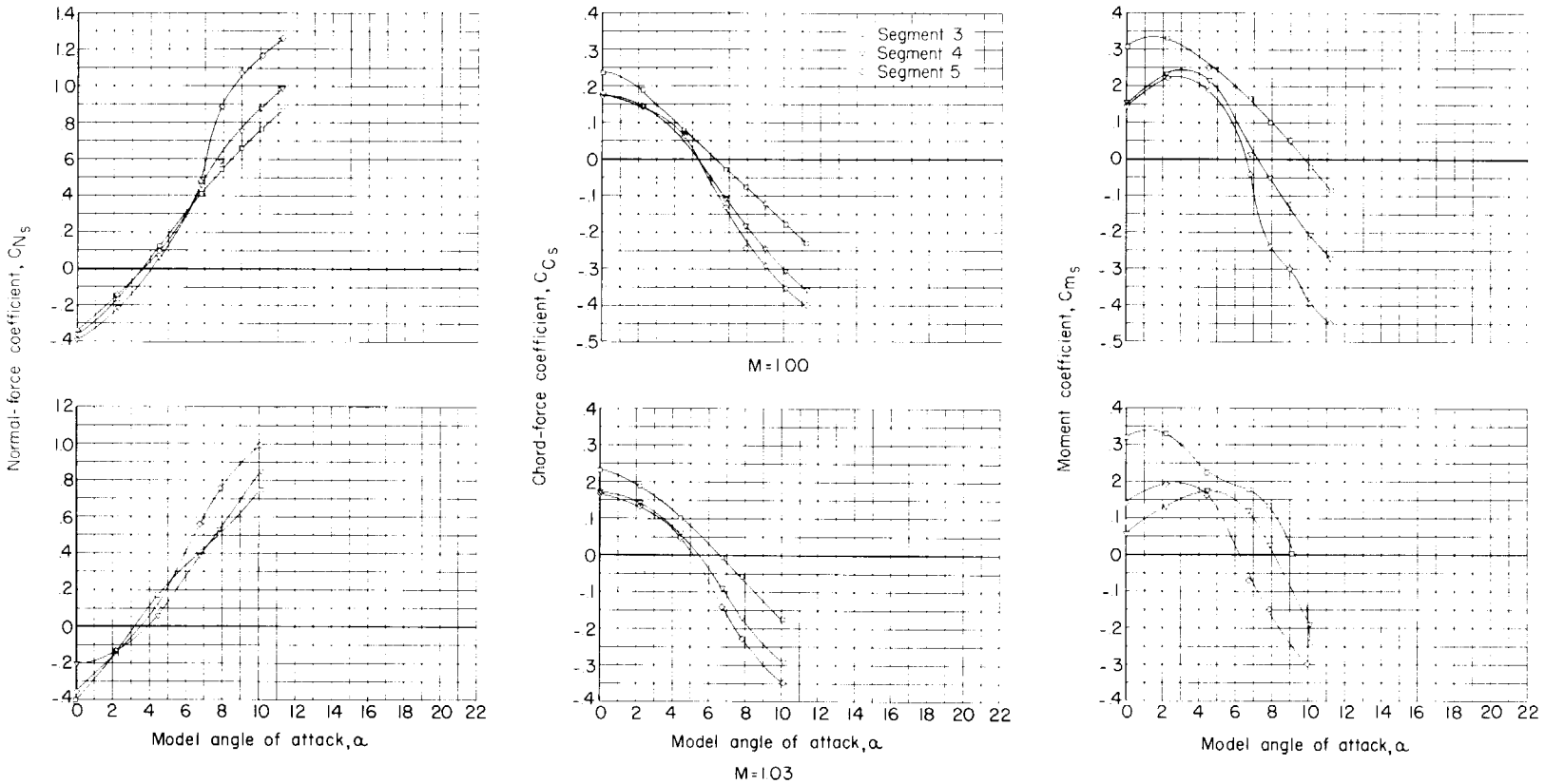

(d) M = 1.00 and M = 1.03.

Figure 7.- Concluded.

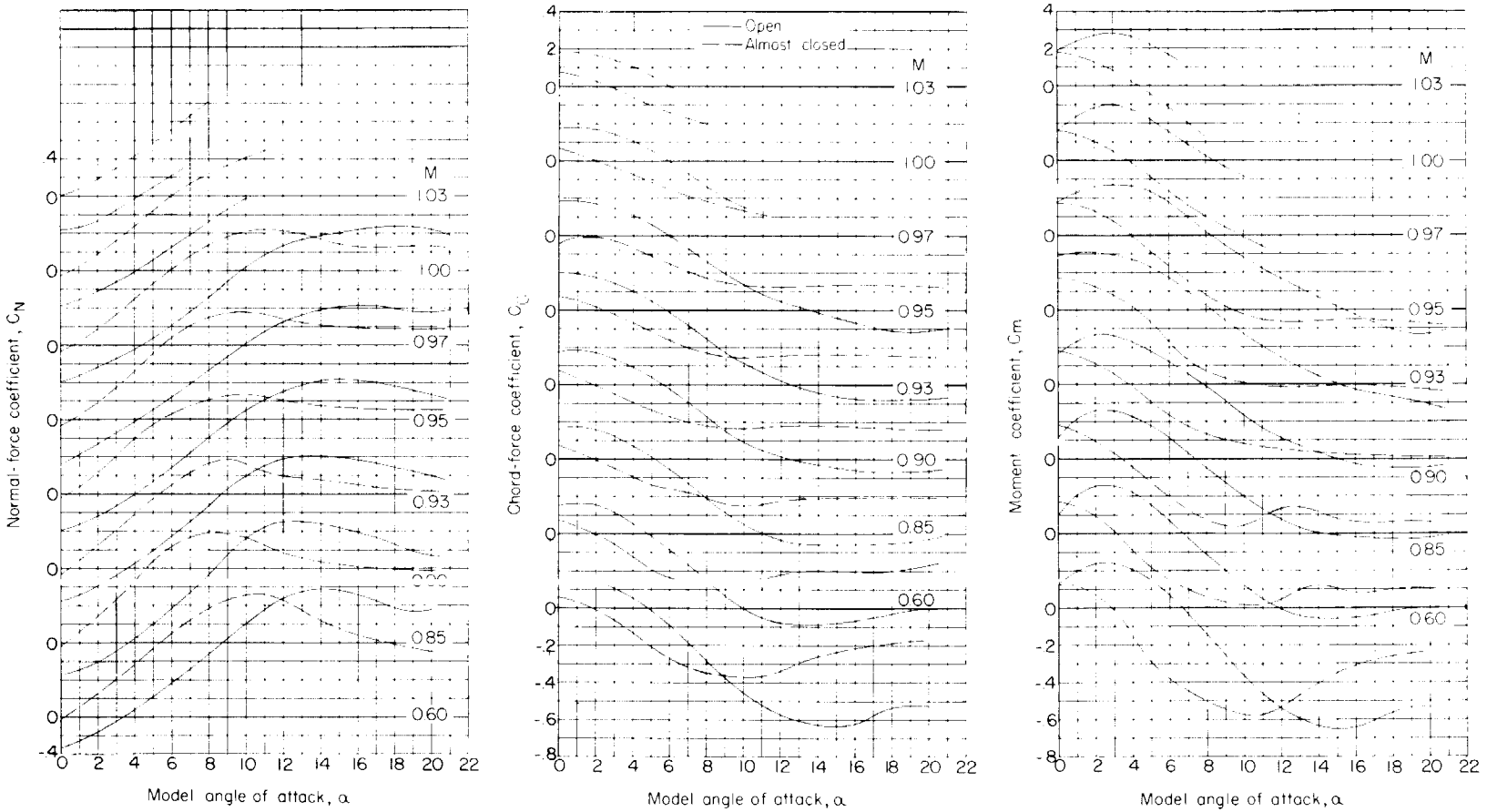

(a) 35- to 95-percent-semispan slats.

Figure 8.- Total slat coefficients for open and almost-closed positions.

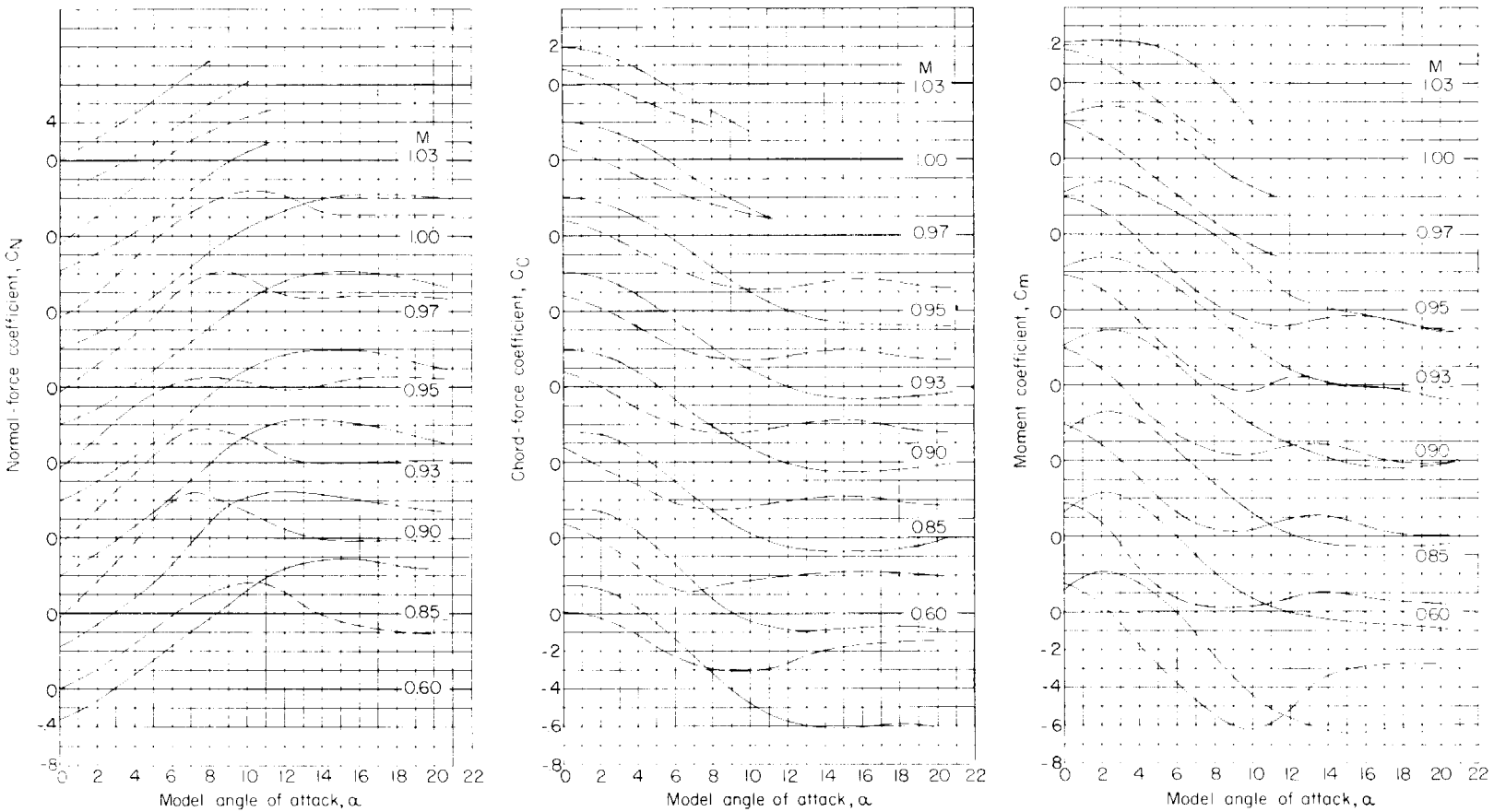

(b) 46- to 95-percent-semispan slats.

Figure 8.- Concluded.

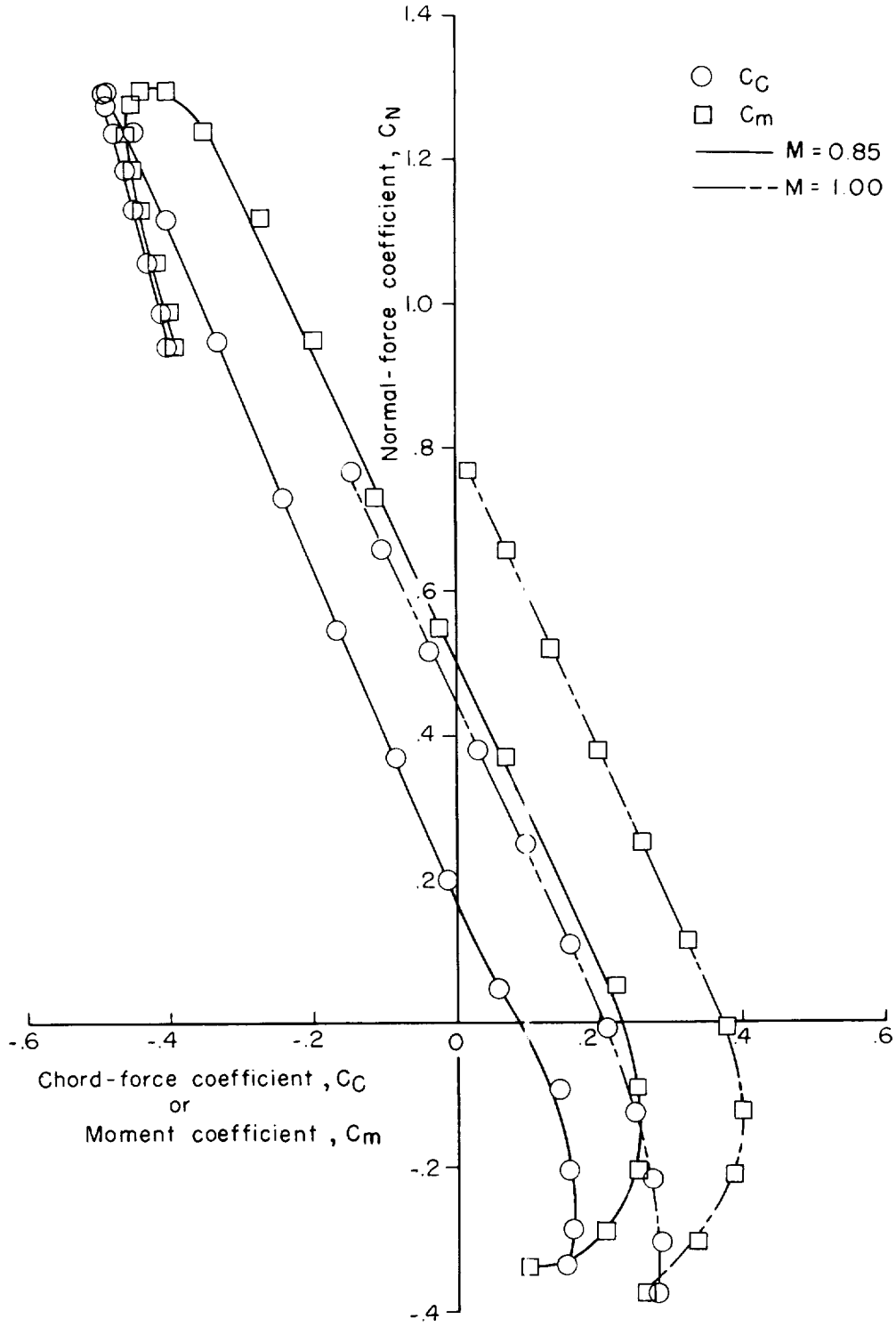

Figure 9.- Variation of normal-force coefficient with chord-force coefficient and moment coefficient for the 35- to 95-percent-semispan slats open.

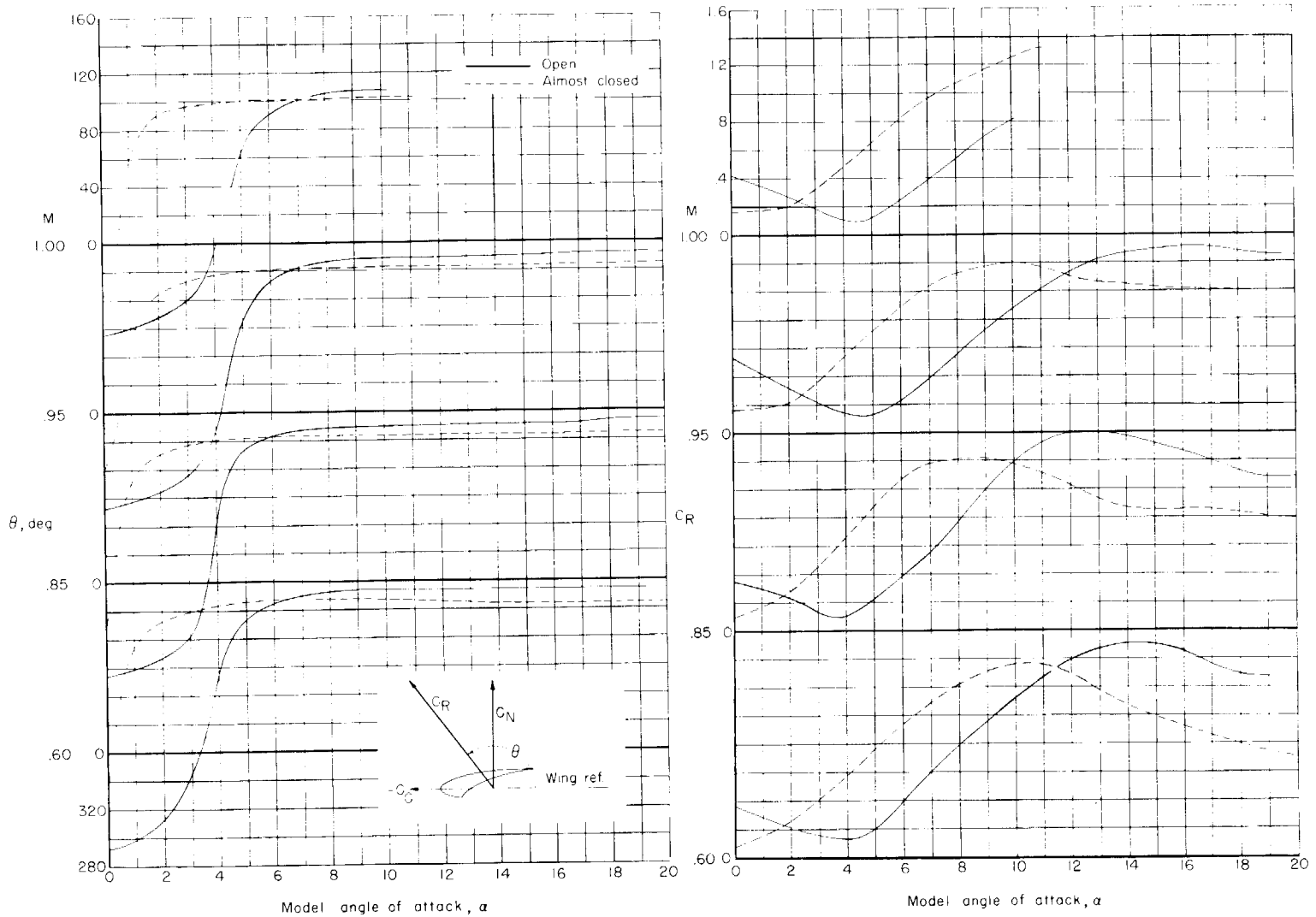

Figure 10.- Magnitude and direction of total resultant-force-coefficient vector for the 35- to 95-percent-semispan slats.

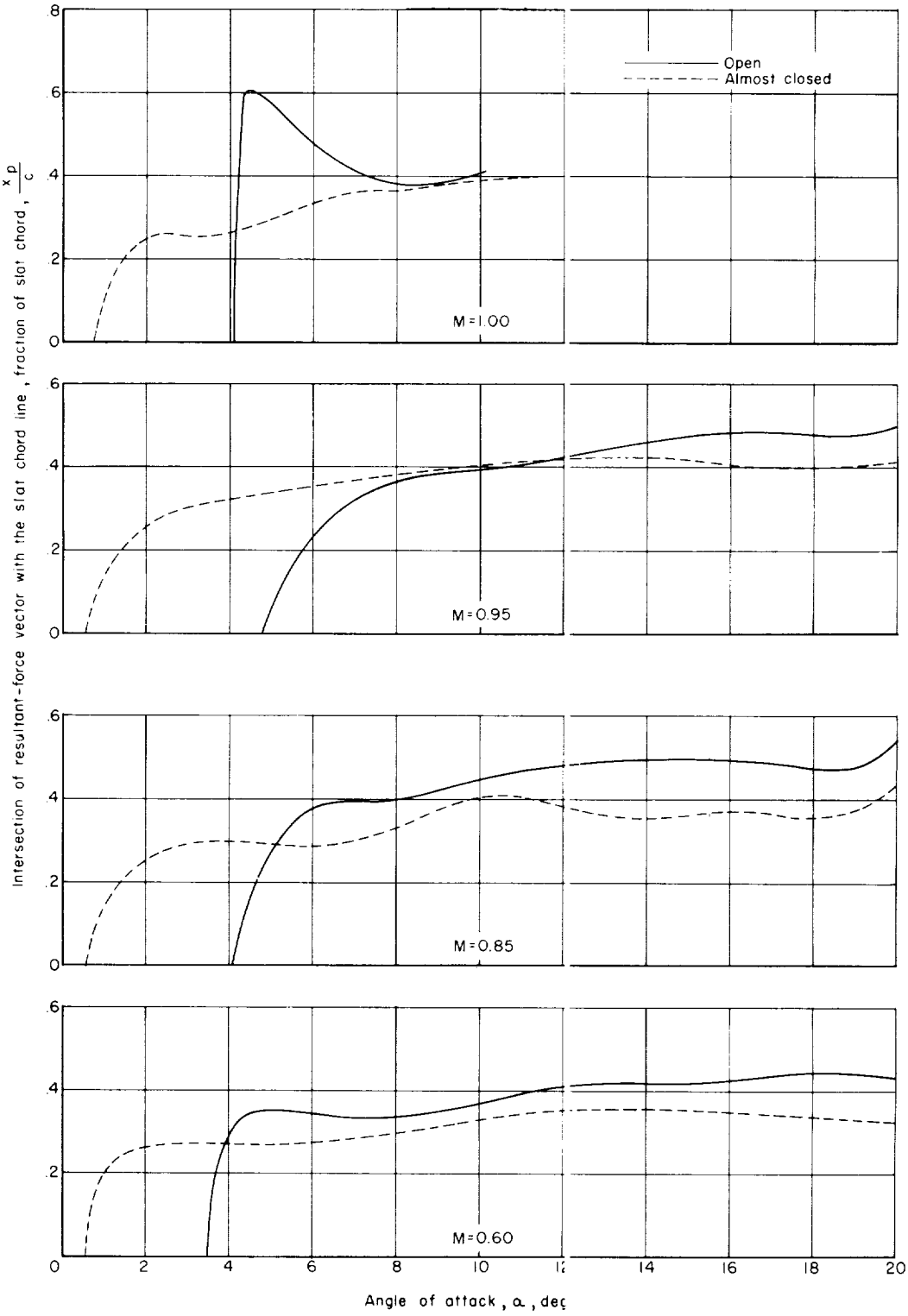

Figure 11.- Intersection of resultant-force vector and slat chord line for the 35- to 95-percent-semispan slats.

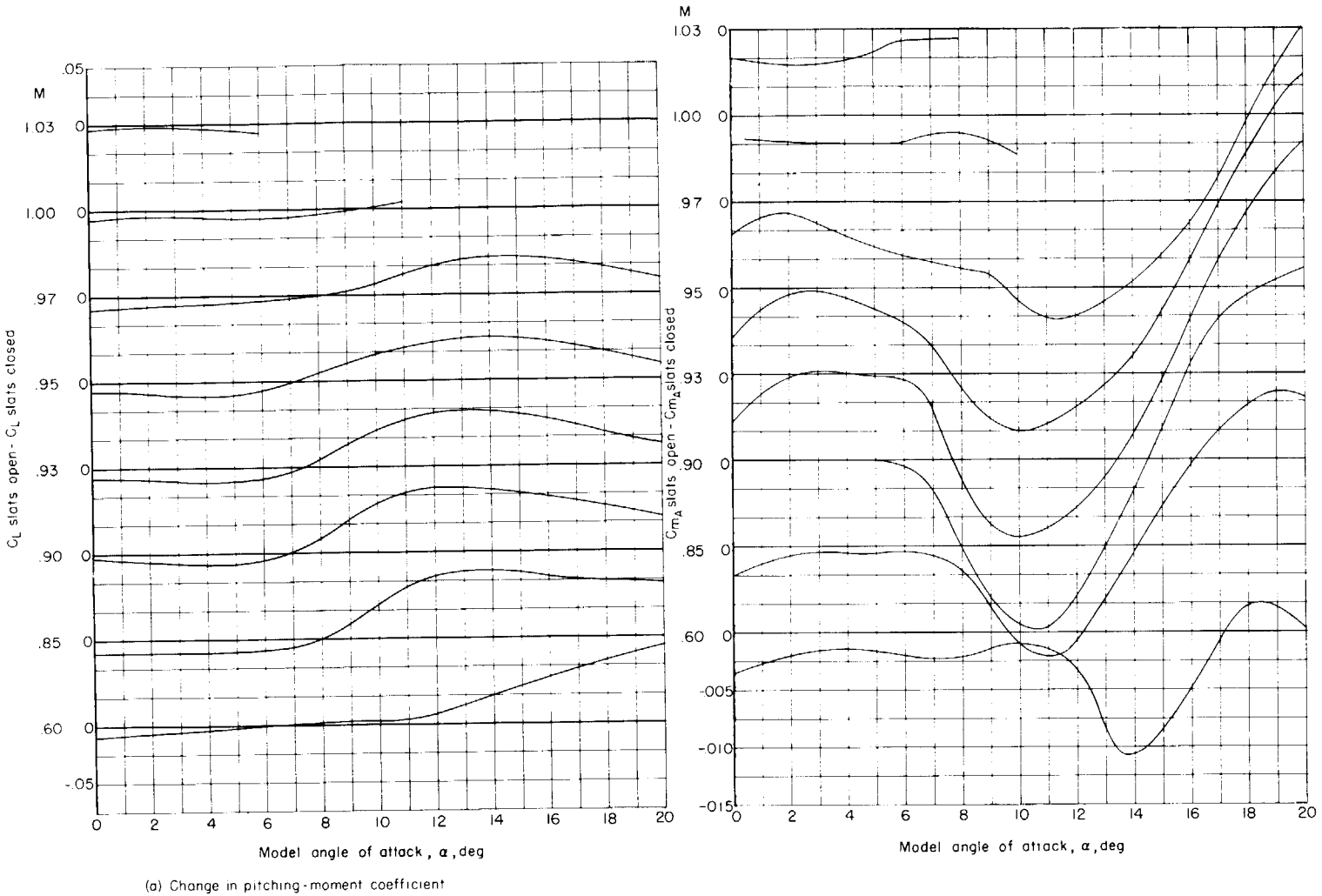

(a) Change in lift and pitching-moment coefficients.

Figure 12.- Change in model aerodynamic characteristics due to opening of 35- to 95-percent-semispan slats.

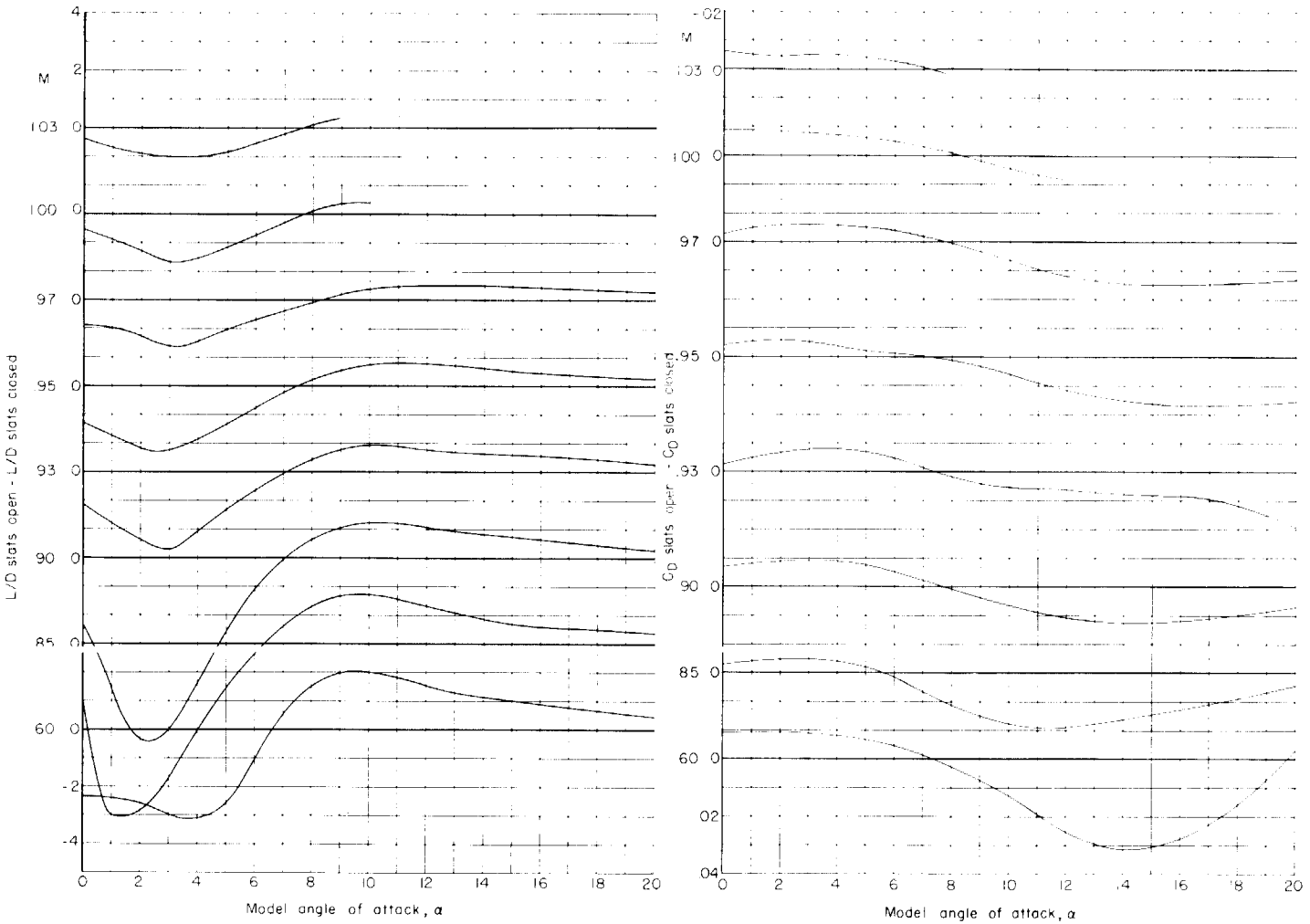

(b) Change in lift-drag ratio and drag coefficient.

Figure 12.- Concluded.

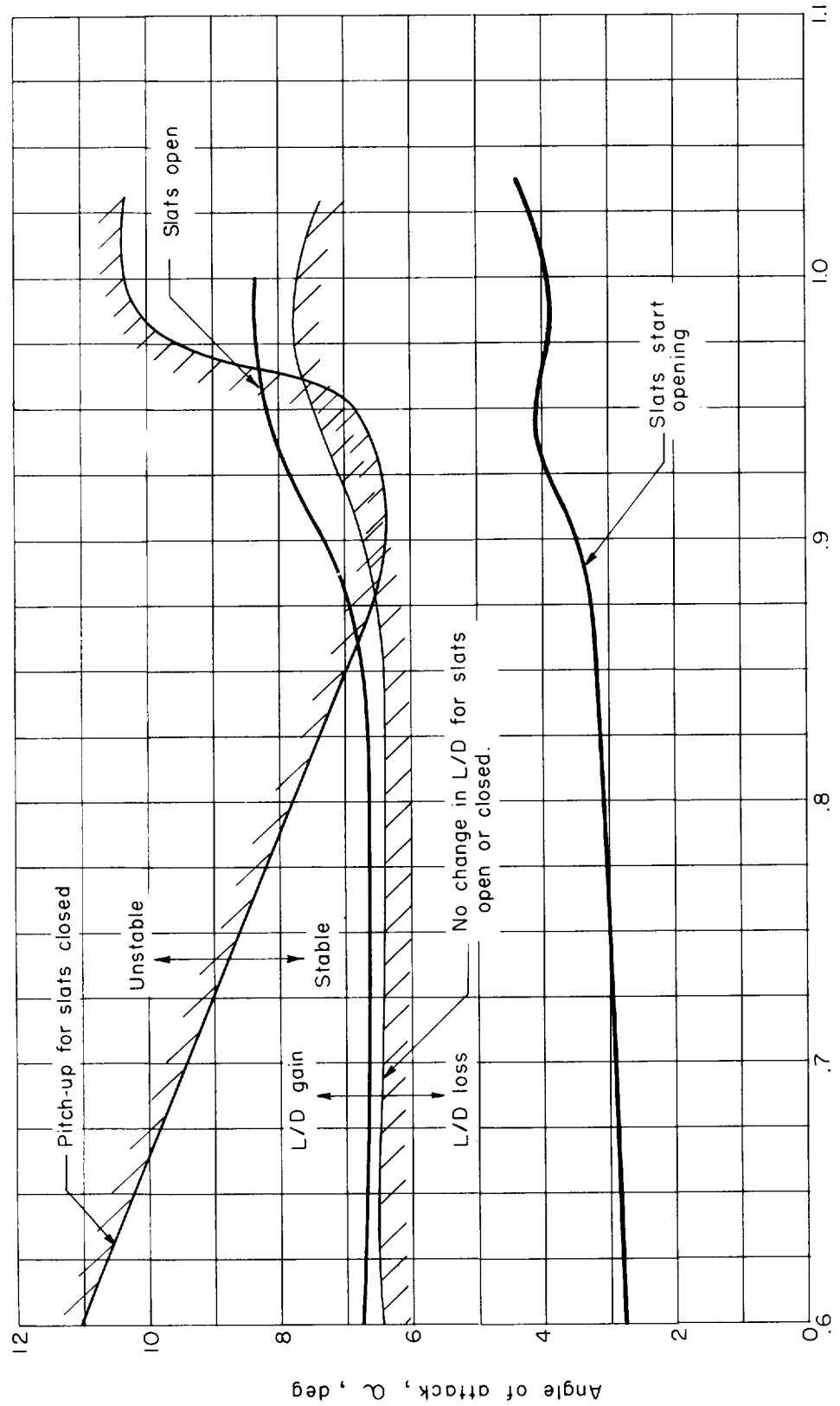

Figure 13.- Angle-of-attack regions where slats start to open and where a gain in aerodynamic characteristics was indicated with slats open.

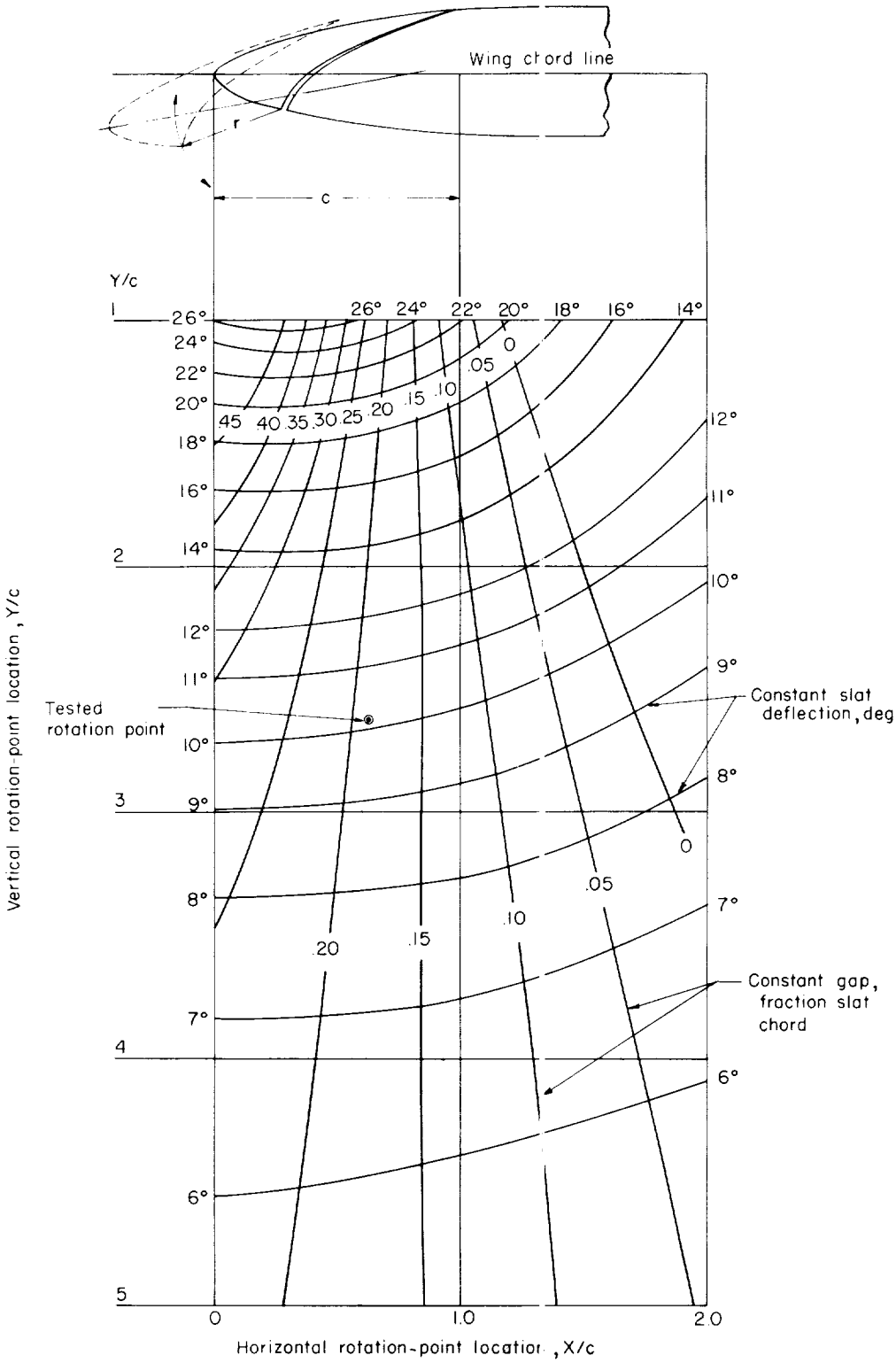

Figure 14.- Variation of slat deflection and gap with rotation-point location; r held constant.

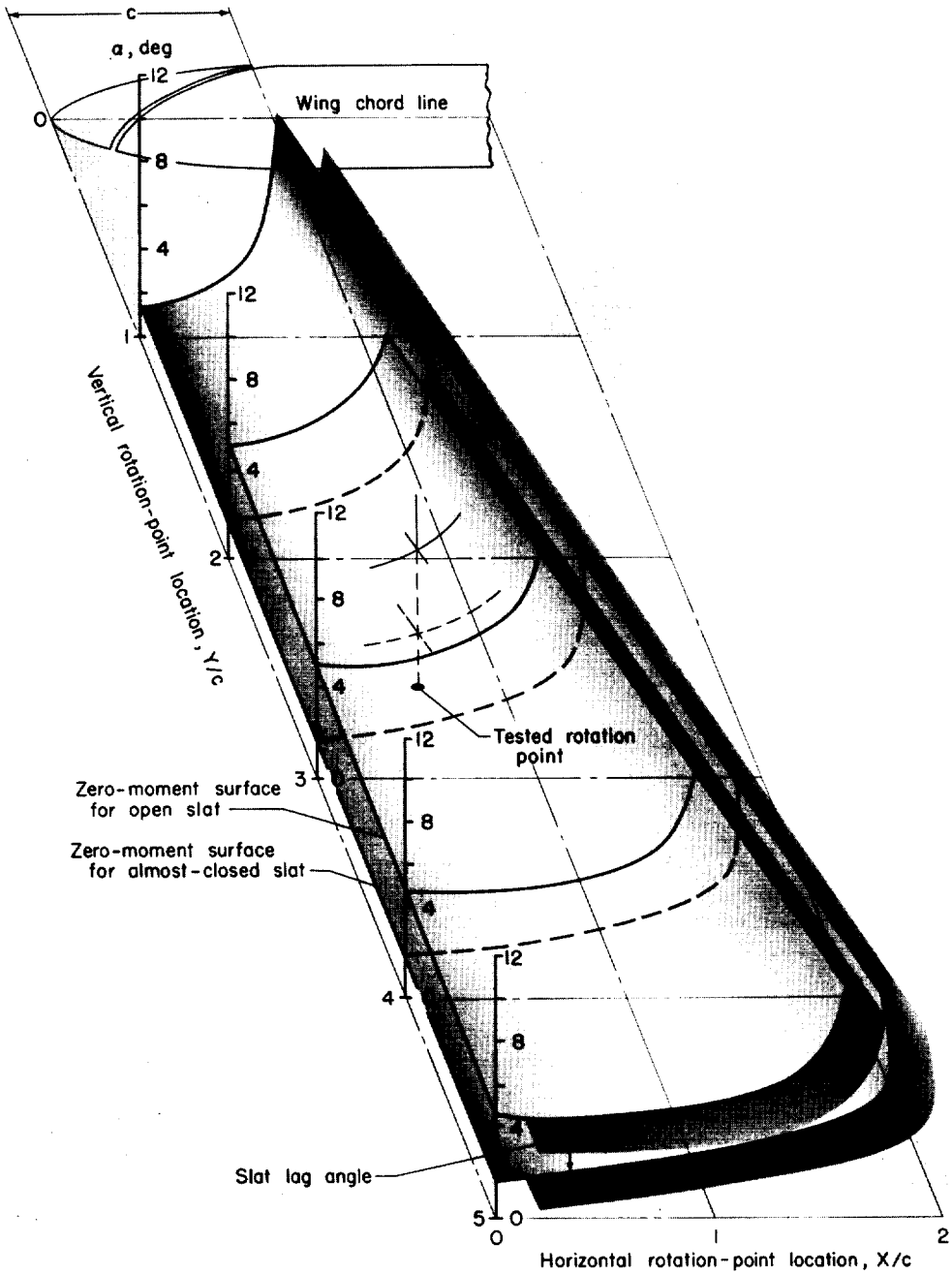

(a) Mach number 0.60.

Figure 15.- Zero-moment surfaces for open and almost-closed slats.

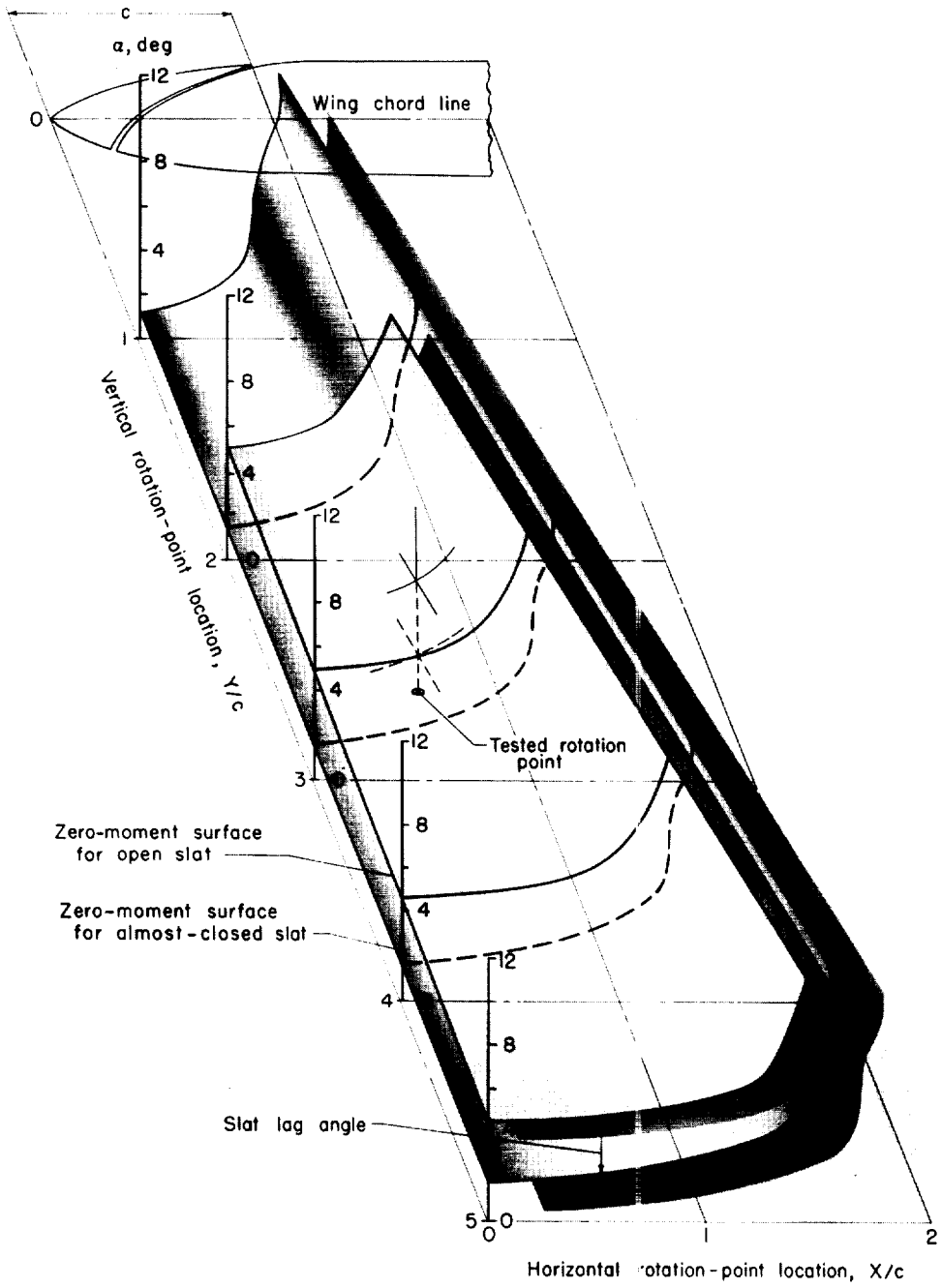

(b) Mach number 0.85.

Figure 15.- Continued.

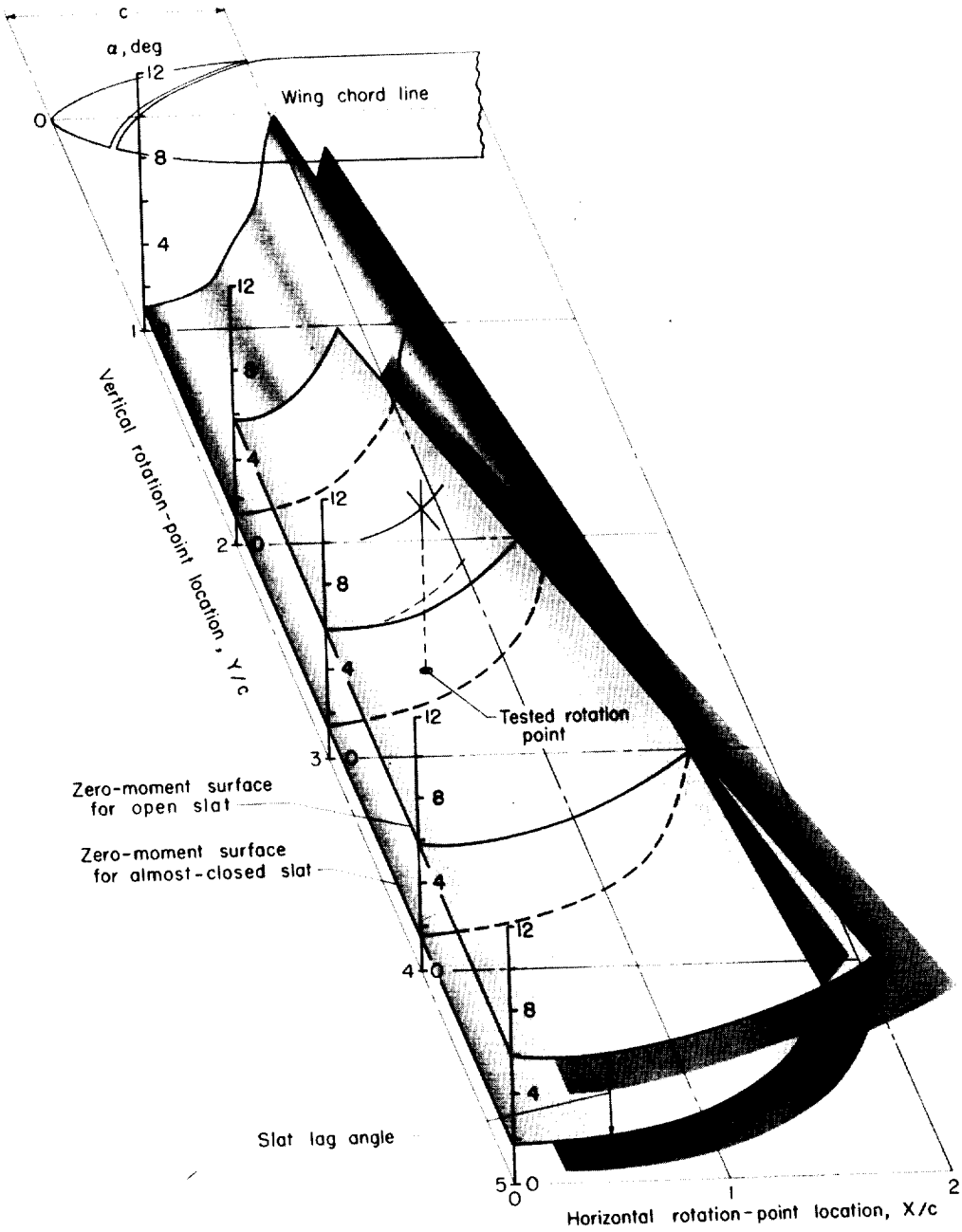

(c) Mach number 1.00.

Figure 15.- Concluded.

NASA-Langley, 1961 L-1609